ENGINEERING EXPERIMENT STATION
DEPARTMENT OF MECHANICAL
AND INDUSTRIAL ENGINEERING
ME-TN-242-3

AN EXPERIMENTAL AND THEORETICAL INVESTIGATION OF THE THERMAL CONTACT RESISTANCE

by
A. M. CLAUSING

Research Sponsored by
NATIONAL AERONAUTICS AND SPACE ADMINISTRATION
under Grant NsG-242-62
FINAL REPORT

UNIVERSITY OF ILLINOIS
URBANA, ILLINOIS
JULY, 1966

ME Technical Report 242-2

July, 1966

An Experimental and Theoretical Investigation of the Thermal Contact Resistance

by

A. M. Clausing

Research Grant No.

NASA NsG 242

FINAL REPORT

Department of Mechanical and Industrial Engineering

University of Illinois

Urbana, Illinois

Acknowledgment

This research was sponsored by the National Aeronautics and Space Administration under Grant NsG-242. The author sincerely appreciated this financial support which substained the research over the past four years.

The author would also like to express his thanks to the many students who at one time or another helped with various phases of this research, particularly, Messrs. R. O. McNary, L. S. Cheema, and B. W. Spencer. Mr. McNary is extending the deformation model which should contribute greatly to the present analysis. Mr. Cheema performed many of the calculations and helped with the design and construction of the new experimental facility.

Foreword

The research summarized in this report was conducted during the last four years with the financial support of the National Aeronautics and Space Administration under Research Grant No. NsG-242-62.

The majority of the research performed has been reported in detail in References 1 through 4 (see Section 6). These reports and journal articles are available to interested readers; therefore, this final report will not attempt to repeat the many data and results which were reported in these references. Instead, an attempt will be made to summarize the results and contributions and give the finer details only for the later extensions which were not reported in these references.

Table of Contents

Nomenclature

a	radius of a contact area, inches
b	radius of constriction region, inches
d	equivalent flatness deviation, inches
E	modulus of elasticity, lbf/in^2
h	interface conductance, $h = \frac{1}{A_a R}$, $BTU/hr\text{-}ft^2\text{-}^oF$
k	thermal conductivity, $BTU/hr\text{-}ft\text{-}^oF$
L	length of specimen, inches
ΔL	equivalent length of contact resistance, inches
p	contact pressure, lbf/in^2
q	rate of heat flow, BTU/hr
r	radial coordinate ($r^* = r/b$)
R	resistance, $^oF\text{-}hr/BTU$
R^*	dimensionless resistance, $\frac{R\,k\,A_a}{b}$
ΔT	a temperature difference, ^oF
x	constriction ratio, $x = a/b$
z	axial coordinate
α	coefficient of linear expansion, $in/in\text{-}^oF$
ζ	elastic conformity modulus, $(\frac{p_a}{E_m})(\frac{b}{d_t})$
ψ	dimensionless interstitial conductance, $(\frac{k_f}{k_m})(\frac{b}{d_t})$

Subscripts

1	region or specimen 1
2	region or specimen 2
12	direction from metal or region 1 to region 2
21	direction from metal or region 2 to region 1
a	apparent contact area
ct	total value when two modes or resistances are important

f	interstitial substance
L	macroscopic constrictions or contact regions
m	a harmonic mean value
o	film resistance
s	microscopic constrictions or contact areas

1.0 Introduction

It is a well recognized fact that the interface between members in contact gives rise to a resistance to the flow of heat from one member to another. This resistance will often dominate the resistance of conductive paths, especially in the case of apparatus located in a vacuum environment. The investigation of the thermal contact resistance in a vacuum environment has been the subject of this study.

Five years ago there was a dearth of data on the thermal contact resistance in a vacuum environment, although a fair amount of information on this resistance for interfaces in air was available. These data were of little value to the space scientist because our inadequate understanding of the problem prohibited his utilization of the available data in his related application.

Today there exist in the literature a large amount of data from investigations of the thermal contact for "realistic engineering type surfaces" in vacuum environments. However, in a large majority of these investigations little was obtained besides numbers representing what was thought to be the thermal resistance of the interfaces. The interfaces were not adequately described, nor could they be since the important parameters were or are unknown; consequently, the measurement represents a unique value for a situation which cannot be repeated and therefore is of little value for making a prediction in an actual apparatus. In short, many data have been obtained at considerable expense, but these investigations of "realistic engineering surfaces" have added little to our understanding of the thermal contact resistance and to our ability to predict the resistance of joints in other physical situations.

On the other hand, the present investigation has not made any attempt to perform tests of realistic engineering surfaces. It was designed with the primary objective of increasing our understanding of the basic mechanisms governing the thermal contact resistance. It is believed that this type of approach will actually result in better success at predicting the resistance of actual interfaces and clearly indicates situations where accurate predictions will be difficult. In essence a better understanding of the importance and effects of the many parameters is obtained, and few problems contain as many variables as are inherent in the thermal contact resistance problem.

A review of the literature on thermal contact resistance is given in Ref. 1. Only a few pertinent references are given in this report. A rather extensive list of references concerned with the subject was compiled by Atkins [5].*

*Numbers in brackets [ ] indicate references listed in Section 7.

2.0 The Mechanism of Heat Transfer at an Interface

The resistance of interfaces is often believed to result in a discontinuity in the temperature distribution at the interface. However, careful measurements usually reveal that the disturbances caused by an interface extend into the region a distance which is comparable to its dimensions. Thus, the resistance in many cases is not a contact resistance but a constriction resistance caused by constricting the heat flow as it passes through the interface. This thermal resistance is often rather loosely defined and carelessly measured which is one of the causes of discrepancies.

In general, a thermal resistance can only be evaluated between isothermal surfaces bounding an imaginary adiabatic heat flow tube. The thermal resistance between two such isothermal surfaces A_1 and A_2 is by definition:

$$R = \frac{|T_1 - T_2|}{k \int_{A_1} \left|\frac{\partial T}{\partial n}\right| d A_1} \qquad (2.1)$$

where n is the normal to the surface and k the thermal conductivity. Let us assume that the region bounded by A_1, A_2 and the heat flow tube is continuous, i.e., free from interfaces or non-perfect joints. If this stream tube is then cut by a surface of area A_a which represents a non-perfect contact between two members such that A_1 and A_2 remain isothermal surfaces, the thermal contact resistance is by definition (see also Figure 2.1)

$$R = \left[\frac{|T_1' - T_2'|}{k \int_{A_1} \left|\frac{\partial T}{\partial n}\right| d A_1} \right]_{\substack{\text{a non-perfect} \\ \text{interface of} \\ \text{area } A_a}} - \left[\frac{|T_1 - T_2|}{k \int_{A_1} \left|\frac{\partial T}{\partial n}\right| d A_1} \right]_{\substack{\text{perfect contact} \\ \text{over area } A_a}} \qquad (2.2)$$

A_a is referred to as the apparent contact area. In many cases a simpler expression for the thermal contact resistance is employed which is:

$$R = \frac{\Delta T}{q} = \frac{1}{h A_a} \qquad (2.3)$$

where q is the total rate of heat flow in the heat flow tube, ΔT is the additional temperature drop between isothermal surfaces A_1 and A_2 due to the presence of the interface of area A_a and h is the interface conductance.

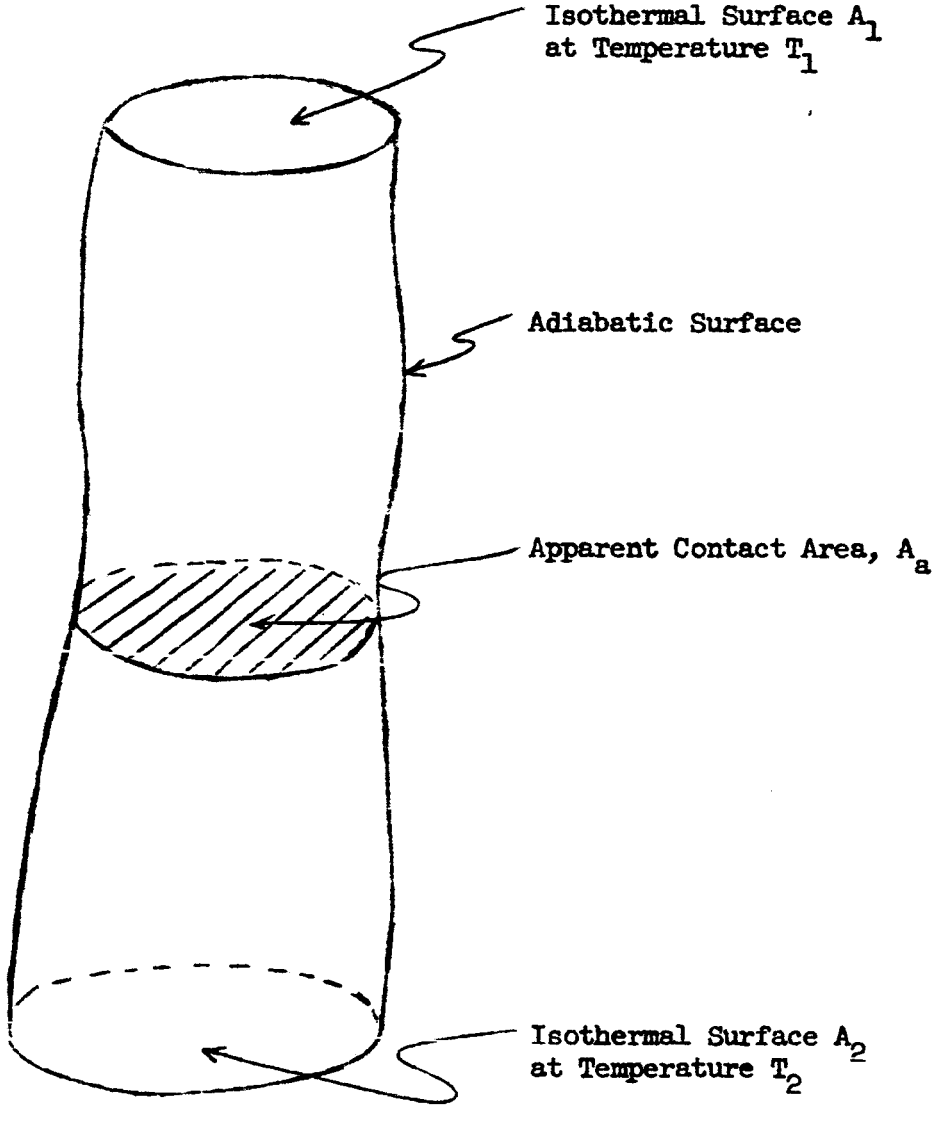

Figure 2.1 A Stream Tube

It is often referred to in the literature and is similar to the surface coefficient of heat transfer employed in convection. The thermal contact resistance is not a property and cannot be tabulated. The effect of an interface is highly dependent on the thermal and physical boundary conditions. Changes in the thermal boundary conditions can also vastly effect the macroscopic conformity of the mating surfaces and consequently the importance of the interface. These effects are discussed in greater detail in Sections 3.6 and 4.2.

Heat is transferred cross an interface by three different modes: (i) thermal radiation, (ii) interstitial conduction, and (iii) metal-to-metal conduction. These three modes are not independent and all modes of importance must be considered simultaneously. It can be easily shown (see Ref. 1) that the contribution of thermal radiation is negligible for metallic interfaces at realistic contact pressures. Furthermore, interfaces in a vacuum environment are of primary interest in this investigation; thus the absence of an interstitial material will be initially assumed. An understanding of the effects of interstitial materials is, of course, also of importance; therefore this problem will be considered after the analysis of the metal-to-metal conduction mode is given. It is logical to consider the simpler, single mode problem before the more complicated case of two interdependent modes.

3.0 A Restrictive Theoretical Model for Prediction of Thermal Contact Resistance

Assuming that the heat transferred across the interface by radiation is negligible and that no interstitial material is present, heat can flow across the interface only through the "points" of contact.

Geometrically flat, smooth surfaces are nonexistant. Real surfaces are characterized by surface roughness, i.e., microscopic irregularities, and flatness deviations, i.e., macroscopic irregularities. Even if an isothermal member had a surface free of microscopic and macroscopic irregularities, it would generally not remain in this condition if heat were flowing through it. An enlarged section of the interface formed by two members in contact would reveal that a relatively small percentage of the surface is in actual contact. When heat flows through an interface it is constricted to these small areas of contact. This constriction manifests itself as a thermal contact resistance at the macroscopic level.

For the purpose of analysis, the apparent contact area was conceived to be divided into two regions: the contact region and the noncontact region. The noncontact region was defined as the portion of the interface which contained few or no microscopic contact areas. The contact region, referred to as the macroscopic contact area, is the portion of the interface where the density of the microcontacts is high. In the absence of a conducting fluid, the flow of heat is first constricted to the macroscopic contact areas; it is then further constricted to the microscopic contact areas within this macroscopic area; and finally it must flow through the surface films. Hence, the total contact resistance for an interface in the absence of an interstitial material such as air may be thought of as the sum of three resistances in series: the macroscopic constriction resistance R_L, the microscopic constriction resistance R_s, and the film resistance R_o, i.e.,

$$R_t = R_L + R_s + R_o \,. \qquad (3.1)$$

It will later be seen that the resistances in Equation (3.1) are not independent. In fact, since a resistance can only be defined between isothermal planes, only the total contact resistance can be defined. The equation is suggested as a help in understanding the problem rather than as an aid in the analysis. Each resistance in Equation (3.1) will now be considered independently.

Microscopic Constriction Resistance

The models proposed in the literature invariably included the assumption that the microscopic contact areas are uniformly distributed over the entire apparent contact area. That is, they analyzed only the microscopic resistance. Let us briefly consider the assumptions which were usually employed and the type of expression which resulted.

It was generally assumed that: (i) the actual areas of contact are uniformly distributed over the entire apparent contact area; (ii) the actual contact areas are all circular and of identical radius, a_s; (iii) the asperities deform plastically under the load P such that the average pressure exerted between them equals the microhardness, H, i.e.,

$$A_s = \frac{P}{H} = n_s \pi a_s^2 \,; \qquad (3.2)$$

and (iv) the film resistance is negligible. With these assumptions the theoretical expression for the interface conductance was shown to be [1]:

$$h = \frac{2 a_s k_m n_s}{g(x_s) A_a} \qquad (3.3)$$

where $g(x_s)$ is a constriction alleviation factor. Roess [6] examined the constriction resistance due to an isothermal circular spot of radius 'a' which feeds heat into a coaxial right circular cylinder of radius 'b'. He found the following expression:

$$g(x) = 1 - 1.40925x + 0.29591x^3 + 0.05254x^5 + 0.02105x^7 + \ldots \tag{3.4}$$

in which $x(= a/b)$ is the constriction ratio. This same problem was solved numerically by the author in order to remove the error caused by Roess' approximation (see Section 3.1). By substituting (3.2) into (3.3) one obtains:

$$h = \frac{2}{\pi} \frac{p_a}{\zeta H} \frac{k_m}{a_s\, g(x_s)} \tag{3.5}$$

The factor $(0 < \zeta < 1)$ was suggested by Holm [7] to account for the elastic deformation between asperities.

The several models employed in the literature all led to expressions similar to Equation (3.5), but little success was obtained with it in predicting the interface conductance. It is not believed, however, that one could expect successful predictions for actual surfaces with the assumption of a uniform distribution of the contact areas--an assumption far from reality for engineering surfaces. The next question which arises is: could such an expression be employed if the condition of macroscopic conformity were satisfied? It is the opinion of the author that one could never accurately estimate the microscopic resistance for an interface in a vacuum in the absence of interstitial materials. The basis for statement follows.

The first difficult question which arises for interfaces in a vacuum

without an interstitial material is what is the "actual" contact area, i.e., what is the effect of gaps of several angstroms or of a discontinuity in the crystal lattice? Also, how important are thin oxide films? Can electrons tunnel across these films and through small gaps? If a material is present which completely fills the interstitials, these difficulties disappear and all gaps of several microinches or less can be considered as a perfect contact for all practical purposes.

Another feature of thermal contacts which adds considerable complexity to the microscopic model is the transient nature of thermal contacts. Whenever the temperature level of one of the members is changed, relative motion between the contacting surfaces occurs. In addition several tests which were performed revealed oscillation in the temperature drop across the interface. A protuberance may be plastically deformed at the first encounter with its mating surface; however, subsequent differential, lateral motion would cause an increase in the contact area. Eventually the load may be borne entirely by elastic deformation.

Finally an estimate of the size and number of microscopic contact areas is required. Even if the total microscopic contact area is constant and macroscopic irregularities are not present, the constriction resistance is highly dependent on the number (or size) of the contact areas. The surface roughness values which are employed in the analysis of thermal contact resistance should give greater weight to the large asperities. The average slope of asperities is also of importance since the constriction ratio and the number of contact areas must be known. Profilemeter traces often mislead one to believe that the asperities have large slopes due to the large vertical magnification relative to the horizontal magnification. In reality, asperity slopes are usually small.

Film Resistance

The magnitude and importance of the film resistance is also hard to predict for many of the same reasons that the microscopic constriction resistance is difficult to estimate. The insulating effect of surface films is known to cause severe disturbances in electrical contacts since their electrical conductivity is vastly different than the base metal. However, the thermal conductivities of the oxide and base metal are not vastly different and consequently their importance is usually discounted. For freshly machined joints in the presence of a conducting fluid, neglecting film resistance is probably justified; however, the heat flow through an interface in a vacuum is confined to relatively small areas which results in a large heat flux through these areas. Sufficiently thick films may also prevent conduction across small gaps by the tunnel effect. Therefore surface films could be of importance for interfaces in a vacuum environment.

With our present insufficient knowledge of the formation and growth of films, their tenacity and ability to withstand load together with the lack of adequate information on the nature of "actual" contact, a theoretical estimation of their importance in thermal contact resistance cannot be made. It is felt that at the present time their influence can more easily be assessed experimentally.

Macroscopic Constriction Resistance

For the purpose of analysis, the macroscopic contact area was assumed to consist of a single circular contact area of radius a_L whose center coincides with that of the apparent contact area which is a circle of radius b_L. (Cylindrical specimens 1" in diameter were employed in the experimental study.) The size of the macroscopic contact area is governed

by the elastic deformation of the contacting members. The flatness deviation or waviness which gives rise to this resistance was simulated by spherical caps of radius r on the end surfaces of the cylindrical contacting members. The length of the cylindrical contacting members, L, was assumed to be large compared with the radius, b_L. The heat flux and the stress was assumed to be uniform and normal to the interface at a distance sufficiently removed from the interface.

The flatness deviation for these spherical surfaces is:

$$d_i \simeq \frac{b_L^2}{2r_i} , \quad i = 1 \text{ or } 2 \qquad (3.6)$$

and the total equivalent flatness deviation is defined as $d_t = d_1 + d_2$. It should be noted that the spherical model of the contacting surfaces exaggerates the flatness deviation, i.e., the flatness deviations over the region where contact occurs under normal loads are small compared with the total flatness deviation. For this reason if the equation which is obtained for the spherical model is to be used for the correlation of data for actual engineering surfaces, the flatness deviation d_t should probably be replaced by four times the deviation that is measured. This point is discussed further in Section 3.2.

The determination of the additional temperature drop due to the presence of a constriction consists of two parts: (i) given the load, what is the macroscopic contact area? and (ii) given the macroscopic contact area, what is the constriction resistance? Once the constriction resistance is known, the additional temperature drop due to the presence of the interface can be easily calculated. For the model employed, it is sufficient to determine the

constriction ratio x_L for the solution of Part (i). This ratio was found in terms of the apparent contact pressure p_a, and the harmonic mean modulus of elasicity E_m as:

$$x_L = 1.285 \left[\left(\frac{p_a}{E_m}\right) \left(\frac{b}{d_t}\right) \right]^{1/3}, \quad \left\{ \begin{matrix} L/b > 2.0 \\ x_L < 0.65 \end{matrix} \right\} \qquad (3.7)$$

The dimensionless group $\left(\frac{p_a}{E_m}\right) \left(\frac{b}{d_t}\right)$ was designated by ζ and called the elastic conformity modulus. It is a measure of the conformity of the mating surfaces under load. Equation (3.7) is basically the Hertz solution. It assumes elastic deformation between the contacting members (which is satisfied in this problem) and further that the radius of the contact area is small compared with the other dimensions of the region. This condition is satisfied only for small values of x_L. In addition, Hertz solution cannot be employed for geometries other than spherical or cylindrical ones. Section 3.2 gives a discussion of an investigation under progress which is designed to eliminate these severe restrictions.

The solution of Part (ii) is similar to the microscopic problem. A dimensionless constriction resistance will be defined as:

$$R^* = \frac{k_m R A_a}{b_L} = \frac{\Delta L_m}{b_L} \qquad (3.8)$$

which is equal to $\frac{k_m}{hb}$ for the present geometry where $k_m \left(= \frac{2 k_1 k_2}{k_1 + k_2}\right)$ is the harmonic mean thermal conductivity. ΔL_m may be interpreted as an equivalent length of the contact resistance. Again employing Roess' solution (see Eq. 3.4) gives:

$$R^* = \frac{k_m}{h b_L} = \frac{\pi g(x_L)}{2 x_L} = \phi(\zeta) \qquad (3.9)$$

where

$$\phi(\zeta) = \frac{(2)(1.285\ \zeta^{1/3})}{\pi g(1.285\ \zeta^{1/3})}, \quad \left\{ \begin{matrix} L/b > 2.0 \\ \zeta < 0.06 \end{matrix} \right\} \quad (3.9a)$$

Roess' approximate solution was found to be accurate for small values of $x_L < 0.5$ ($\zeta < 0.06$). A more accurate solution to this problem is given in Section 3.1 which relaxes the stringent condition on Equation (3.9a). It is to be noted that the solution is valid for dissimilar metals in contact only if the effects of thermal strain are negligible (see Ref. 4).

It is seen that for the restrictive model being employed, the macroscopic constriction resistance can be accurately calculated and all parameters required for this calculation can be easily determined. Employing Equations (3.5) and (3.9), estimates of the relative importance of the macroscopic and microscopic constriction resistances were made in Reference 1. These results indicated the macroscopic constriction resistance was several orders of magnitude larger than the microscopic resistance; consequently, the microscopic constriction resistance could be neglected. It is not felt that these results are unquestionable evidence of the lack of importance of microscopic resistances because (i) the microscopic constriction resistance model is of doubtful validity , (ii) the assumed values of unknown parameters in the microscopic model could be in error, and (iii) the importance of film resistances has not been considered. On the other hand, it is believed that accurate estimates of thermal contact resistance in the absence of interstitial materials will only be possible for interfaces where microscopic resistances play a minor role.

The experimental investigation reported in References 1 and 2 gives an indication of the relative importance of microscopic and macroscopic

resistances. These results indicated that in the absence of thick surface films the macroscopic constrictions have a commanding influence for many surfaces commonly encountered in engineering practice. The results are briefly summarized in Section 4.1.

3.1 Extension of Roess' Analysis

The analysis of the thermal constriction problem performed by Roess contained several assumptions which severely limits its usefulness. These assumptions will be removed in the present analysis. Since the results which follow are applicable to both large scale and small scale resistances, the subscripts will be dropped.

One region of the model being considered is shown in Figure 3.1. Only one region is being employed for simplicity; consequently, the problem must be chosen such that it is symmetrical with respect to the contact plane. Symmetry is assured if the radii are identical and the lengths are identical. (The lengths need not be the same if both L_1/b and L_2/b are greater than 1.) The conductivities of the regions can be different. Because the flatness deviation is several orders of magnitude smaller than the other dimensions, the boundary conditions which exist along the curved contact surface may be imposed along the line $z = 0$. Assuming that a perfect contact exists over the region of radius a, the following partial differential equation and boundary conditions describe the temperature field:

$$\frac{\partial^2 T}{\partial r^2} + \frac{1}{r}\frac{\partial T}{\partial r} + \frac{\partial^2 T}{\partial z^2} = 0 \qquad (3.10)$$

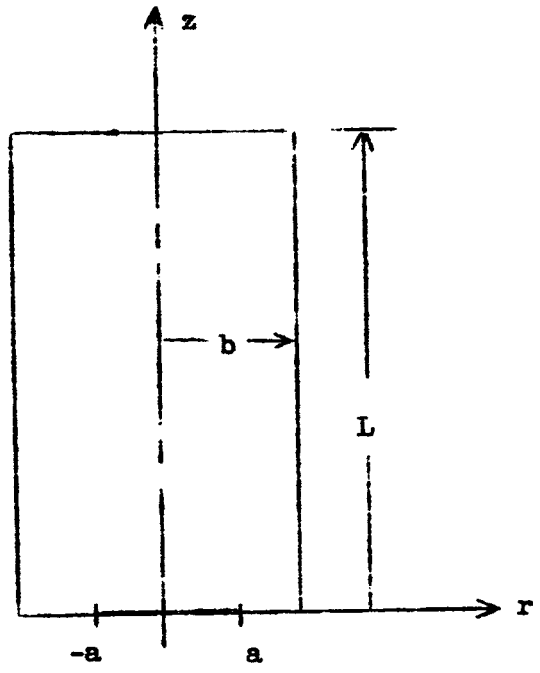

Figure 3.1
Finite Cylindrical Region

$$T(r,o) = T_o, \qquad 0 \le r \le a \qquad (3.10a)$$

$$\frac{\partial T}{\partial z}(r,o) = 0, \qquad a < r \le b \qquad (3.10b)$$

$$\frac{\partial T}{\partial r}(b,z) = 0, \qquad 0 < z < L \qquad (3.10c)$$

$$T(r,L) = T_L, \qquad 0 \le r \le b \qquad (3.10d)$$

This problem is a very formidable one due to the mixed boundary condition at $z = 0$. The boundary is isothermal for $0 \le r \le a$, whereas there is zero heat flux over the remainder of the boundary, i.e., for $a < r \le b$. The difficulty due to this mixed boundary condition was circumvented by Roess [6], who found that a flux distribution across the area $0 \le r \le a$ which was proportional to $(1 - r^2/a^2)^{-1/2}$ resulted in an approximately isothermal area unless the constriction ratio x $(= a/b)$ was near unity. In addition, Roess assumed L/b was sufficiently large that the constriction resistance was independent of L/b (see Figure 3.1). With these additional assumptions he found the constriction resistance was:

$$R(x) = \frac{g(x)}{4\,a\,k} \qquad (3.11)$$

where

$$g(x) = 1 - 1.40925\,x + 0.29591\,x^3 + 0.05254\,x^5 + 0.02105\,x^7 + 0.01107\,x^9 + \ldots$$

and k is the thermal conductivity. This solution was employed in the analysis given in [1]. The experimental data were then compared with the resulting theoretical prediction.

Further analysis of this was deemed highly desirable since:

(i) Roess' solution failed is $L/b < 1$. This region is probably the most important one, especially in the study of thermal contact resistance problems connected with space vehicles where thin plates are often employed. Under such circumstances, small values of L/b would be present and the theoretical prediction of [1] would no longer be applicable.

(ii) The theoretical solution of [1] which employed Roess' solution predicted smaller values of the constriction resistance than the experimental values if x was near unity. Part of this discrepancy could be due to the failure of Roess' solution to apply, since his assumed flux distribution is in error if x is near unity.

The problem described by equations 3.10 was solved numerically. The justification of a numerical procedure, the details of the numerical techniques including the appropriate difference relationships, and a detailed presentation of the results of these calculations are given in Ref. 3. For the readers' convenience, the results are repeated in this report in Tables 3.1 and 3.2. Tables 3.1 and 3.2 gives the dimensionless constriction resistance as defined by Equation (3.8) and are the constriction resistance of one region only. The data of Table 3.1 for the case of $L/b > 0.8$ were fitted with a fifth degree least squares polynominal. The resulting equation is:

$$R^* = \frac{\Delta L}{b} = 10^{f(x)} , \quad \left\{ \begin{matrix} L/b & > 0.8 \\ .16 < x < .84 \end{matrix} \right\} \tag{3.12}$$

$R^* = \Delta L/b$

L/b \ x	.167	.233	.300	.367	.433	.500	.567	.633	.700	.767	.833
0.0	0	0	0	0	0	0	0	0	0	0	0
.0667	1.689	0.906	.552	.360	.247	.173	.122	.0856	.0589	.0389	.0231
.1333	2.542	1.446	.911	.6080	.4216	.2970	.210	.1460	.0990	.0630	.0352
.200	3.000	1.772	1.145	.7760	.5425	.3830	.270	.1816	.1240	.0765	.0407
.267	3.257	1.972	1.299	.8878	.6237	.4410	.3090	.2115	.1387	.0836	.0434
.4	3.494	2.169	1.452	1.006	.7105	.5014	.3495	.2360	.1522	.0897	.0452
.6	3.597	2.258	1.526	1.063	.7523	.5306	.3680	.2470	.1575	.0919	.0459
.8	3.618	2.277	1.542	1.077	.7615	.5368	.3720	.2493	.1584	.0923	.0459
1.0	---	2.281	1.544	1.080	.7636	.5380	.3728	.2498	.1585	.0924	.0460
1.2	---	---	---	---	.764	---	.3729	---	---	---	---
	3.625	2.283	1.545	1.080	.764	.539	.373	.250	.159	.0924	.0460

Table 3.1 The Dimensionless Constriction Resistance R^* as a Function of x and L/b

$R(L/b) \;/\; R(L/b = \infty)$

L/b \ x	.167	.233	.300	.367	.433	.500	.567	.633	.700	.767	.833
0	0	0	0	0	0	0	0	0	0	0	0
.0667	.466	.397	.357	.333	.324	.321	.327	.342	.370	.421	.502
.1333	.703	.632	.590	.563	.553	.552	.564	.584	.623	.682	.765
.200	.828	.777	.741	.719	.711	.711	.724	.745	.780	.828	.885
.267	.889	.864	.841	.812	.816	.819	.829	.846	.872	.905	.944
.4	.965	.950	.940	.931	.931	.932	.936	.945	.959	.971	.984
.6	.993	.989	.988	.985	.986	.986	.986	.989	.991	.995	.998
.8	.998	.995	.999	.996	.998	.998	.999	.997	.998	.999	.998

Table 3.2 The Ratio $R(L/b) \;/\; R(L/b = \infty)$ as a Function of x and L/b

where

$$f(x) = [1.398386 - 7.446978\ x + 19.93028\ x^2 - 38.58965\ x^3 + 38.65529\ x^4 - 16.62469\ x^5]$$

The dimensionless contact resistance for two similar regions in contact is:

$$R^* = 2(10^{f(x)}), \quad \left\{ \begin{matrix} L/b > .8 \\ .16 < x < .84 \end{matrix} \right\}$$

Thus, Equation (3.9) becomes

$$R^* = \phi(\zeta) \qquad \left\{ \begin{matrix} L/b > 2.0 \\ .002 < \zeta < 0.14 \end{matrix} \right\} \tag{3.13}$$

where

$$\phi(\zeta) = 2\left\{10^{f[1.285(\zeta^{1/3})]}\right\}$$

and R^* is based on the harmonic mean of the thermal conductivities of the two regions.

Roess' solution was found to give good agreement with the numerical results for small values of x (< 0.5); therefore, no attempt was made to obtain numerical results for $x < 0.16$. On the other hand, Roess' solution diverged rapidly at larger values of x, and at $x = 0.8$ it was already in error by approximately 30%.

3.2 Extension of Hertz's Analysis

The flatness deviation in the proposed model was simulated by spherical caps on the ends of the cylindrical regions. This model was ideal for theoretical calculations since:

(i) The Hertz result could be employed in the calculation of the macroscopic contact area. (Hertz solved the classical problem of the determination of the contact area between two spherical bodies of radii r_1 and r_2 in elastic contact. The radius of the contact was given by

$$a = \left[\frac{3P}{4} \left(\frac{1 - \nu_1^2}{E_1} + \frac{1 - \nu_2^2}{E_2} \right) \left(\frac{1}{r_1} + \frac{1}{r_2} \right)^{-1} \right]^{1/3}$$

$$x_L = 1.285 \left[\left(\frac{p_a}{E_m} \right) \left(\frac{b_L}{d_t} \right) \right]^{1/3} \qquad (3.14)$$

which is the expression employed in Section 3.0.); and

(ii) Spherical surfaces which were flat to within several millionth's of an inch could be easily generated. The object of the experimental study was to determine if macroscopic effects would be dominant even for surfaces which were almost optically flat as was indicated from the estimations of the relative importance of microscopic and macroscopic constriction resistances. Also it was desired to determine if film resistances might be of importance for these flat specimens. Since no other surface geometry could be consistently generated with such small, measurable values of flatness deviation, the spherical geometry was a necessity.

It is seen that an accurate theoretical calculation was possible for the spherical model. This model also enabled one to further considerably the understanding of the important parameters since a rather exact experimental representation was possible; thus, it enabled a unified and systematic study of the many perplexing phenomena associated with the thermal contact resistance. Its usefulness and potential can perhaps be better realized from the remainder of the report.

An extension of the results obtained by Hertz is highly desirable since:

(i) Hertz assumed that the dimensions of the bodies in contact were large in comparison with the radius of the boundary of the surface of contact; thus Equation (3.14) is not valid for large values of x_L.

(ii) Hertz's solution is only valid for an isothermal region, i.e., thermoelastic effects are neglected. Thus, a theoretical prediction of the directional effect which is experienced in contacts between dissimilar metals is not possible. (See Section 4.2 or Ref. 4 for a discussion of the directional effect.)

(iii) Hertz's solution is valid only for contacts formed between cylindrical or spherical members. Although a spherical model was convenient for this basic analysis, it does not appear to be the best geometry for the representation of the flatness deviation which occurs for surfaces manufactured by various production techniques.

(iv) If the prediction of the thermal contact resistance for interfaces with an interstitial material is to be made, the distance between the contacting members in the non-contact region and the variation

of this distance with load must also be known. Previously only the size of the contact area was required which could be obtained from Hertz's solution. The need for this extension can be appreciated by an examination of Section 3.4.

The extension of Hertz's solution is being investigated by R.O. McNary. The study when completed will be his Ph.D. thesis. He has formulated the problem in terms of displacement and is solving the resulting coupled partial differential equations using a finite difference technique. This work should be completed in several months at which time the details of this analysis will be available. The numerical results which have been obtained so far still contain appreciable numerical error; therefore they will not be reported at this time.

3.3 The Interdependence of Microscopic and Macroscopic Resistances

In the study of the relative importance of the macroscopic and microscopic resistances it is of interest to know how the macroscopic and microscopic resistances are interrelated. It is seen that they are not independent since the presence of a microscopic resistance would, of course, affect the macroscopic temperature and flux distribution and consequently the macroscopic constriction resistance.

The change in the macroscopic constriction resistance, R_L, if a microscopic resistance, R_s, is uniformly distributed over the macroscopic contact was considered by Holm [7] and also was discussed in [1]. The limiting situations were considered. Holm suggested that if R_s is very large compared with R_L and is uniform over the macroscopic contact area, it followed that the heat flux through the contact region is approximately uniform. He went on to assume the flux was constant and determined the macroscopic constriction

resistance with this boundary condition. Although this boundary condition is approximately true, it cannot be employed in the calculation of R_L, a secondary resistance.

A closer examination of the problem shows that if the two specimens have the same radius b_L and length L and if the distribution of the microscopic resistance is axially symmetric (it is not necessary to assume the distribution is uniform), an isothermal surface exists within the plane of contact. The presence of the microscopic resistance over the boundary is analogous to a convective type boundary condition with a finite surface conductance.* The region shown in Figure 3.1 is again applicable. The differential equation given by (3.10) and the boundary conditions given by (3.10b) - (3.10d) apply; however, the boundary condition which was previously given by Equation (3.10a) now becomes:

$$+ k \frac{\partial T}{\partial z}(r,o) = h[T(r,o) - T_o], \quad 0 \leq r \leq a_L \tag{3.15}$$

where h is a function of r if the microscopic resistance is not uniformly distributed; otherwise, it is a constant. T_o is the temperature of the isothermal surface in the contact plane. The contact resistance in this case is given by:

$$R = \frac{T_L - T_o}{q} - \frac{L}{k\pi b_L^2}$$

*The region of the microscopic resistance is assumed to be of negligible thickness. This assumption is probably a valid one.

where q is the rate of heat flow through the region. The relationship between h and the microscopic resistance, R_s, will now be determined.

Consider two regions of different materials in contact. Assume a known microscopic resistance is uniformly distributed across the macroscopic contact area. (A non-uniform axially-symmetric distribution would add little complication; however, the results would be of less general value.) If one is to consider only one region for the solution of this problem, it is required that the flux distributions across the contact area of each region are identical. From the differential equation and boundary condition it can be seen that this will be the case if the microscopic resistance is partitioned such that

$$\frac{h_1}{k_1} = \frac{h_2}{k_2} \tag{3.16}$$

Also

$$h = \frac{1}{\pi a_L^2 R}; \quad R_s^* = \frac{k_m R_s \pi b_L^2}{b_L} \quad \text{and} \quad R_s = R_1 + R_2$$

Therefore

$$R_1 = R_s \frac{1}{[1 + \frac{k_1}{k_2}]}$$

or

$$h_1 = h_s [1 + \frac{k_1}{k_2}] \tag{3.17a}$$

and

$$h_2 = h_s [1 + \frac{k_2}{k_1}] \tag{3.17b}$$

With the convective type boundary condition Eq. (3.15), the Biot number, $h\, b_L/k$, enters into the solution. In terms of the above quantities, the Biot number can be written as:

$$\frac{h_1 b_L}{k_1} = \frac{2}{x_L^2 R_s^*} = \frac{h_2 b_L}{k_2} \tag{3.18}$$

where R_s^* is based on the summation of the microscopic resistances of both regions.

It is therefore possible to find the total contact resistance between any two mating materials separated by a small scale resistance, R_s, by finding the resistance of one region if the small scale resistance is partitioned as described. The dimensionless contact resistance of both regions will be the same if each is based on its respective thermal conductivity. The total dimensionless contact resistance for two dissimilar regions based on their harmonic mean conductivity then becomes:

$$R_{ct}^* = \frac{(R_1 + R_2)\, k_m\, A_a}{b} = \left\{ \frac{R_1^*}{k_1} + \frac{R_2^*}{k_2} \right\} k_m = 2 R_1^* = 2 R_2^* \tag{3.19}$$

The numerical procedure employed in Ref. 3 in obtaining the solution for the case of negligible microscopic resistance was again used. A difference equation for the boundary $0 \le r \le a_L$ is now required in addition to those given in [3]. In terms of the nomenclature of [3], a general difference equation valid for the grid points on this boundary is:

$$\left(1 + \frac{\Delta r}{2r_i}\right) T_{1,j+1} + 2 T_{2,j} + \left(1 - \frac{\Delta r}{2r_j}\right) T_{1,j-1} + 2 \frac{h_1 b_L}{k_1} \left(\frac{\Delta r}{b_L}\right) T_o - \left\{ 4 + 2 \frac{h_1 b_L}{k_1} \left(\frac{\Delta r}{b_L}\right) \right\} T_{1,j} = 0 \tag{3.20}$$

where the Biot number is given by Equation (3.18).

A series of numerical calculations were made to determine the total dimensionless contact resistance, R_{ct}^*, for the problem as specified for several values of x_L and for several lengths. This solution was compared with the result obtained by adding $R_s^* + R_L^*$. In these calculations, values

of R_s^* and x_L were assumed; R_L^* was obtained from (3.13).

Table 3.3 gives a comparison of these results. The values of all resistances given in the tables are those of one region only; thus, the total contact resistance, for example, for two contacting members is twice the value given in the table. In examining the apparent trends in these values it must be noted that no great effort was expended to remove minor truncation errors since greater accuracy was unnecessary in drawing the desired conclusions. Tables 3.4, 3.5, and 3.6 give the specific values employed in obtaining Table 3.3.

The conclusions which can be drawn from these results are:

1. The total contact resistance of an interface is always greater than the value obtained by assuming R_s^* and R_L^* are independent resistances in series.
2. The error committed by assuming that R_s^* and R_L^* are independent and that the total contact resistance is simply $(R_s^* + R_L^*)$ is small in all cases and, considering the nature of the problem, could easily be neglected.
3. This error vanishes if $R_s^* >> R_L^*$ or if $R_L^* >> R_s^*$.
4. The apparent macroscopic constriction resistance $(R_{ct}^* - R_s^*)$, in the presence of microscopic resistances can differ widely from the value obtained when R_s^* is equal to zero.

Table 3.3 Dimensionless Ratio $\left[\frac{R^*_{ct}}{R^*_L + R^*_s}\right]$

	L/b_L \ x_L	.233	.500	.833
$R^*_s \approx R^*_L$	.200	1.0405	1.0372	1.0704
	.600	1.0454	1.0621	1.0925
	1.00	1.0458	1.0641	1.0891
$R^*_s \approx 10R^*_L$	.200	1.0076	1.0078	1.0214
	.600	1.0112	1.0163	1.0366
	1.00		1.0125	1.0366
$R^*_s \approx .2R^*_L$	.200	1.0466	1.0377	1.0842
	.600	1.0471	1.0520	1.0924
	1.00		1.0533	1.0870

Table 3.4 Comparisons for $R^*_s \approx R^*_L$

L/b_L \ x_L	.233	.500	.833
.200	$R^*_s = 2.281$ $R^*_L = \frac{1.772}{4.053}$ $R^*_{ct} = 4.217$	$R^*_s = .5380$ $R^*_L = \frac{.3830}{.9210}$ $R^*_{ct} = .9553$	$R^*_s = .0460$ $R^*_L = \frac{.0407}{.0867}$ $R^*_{ct} = .0928$
.600	$R^*_s = 2.281$ $R^*_L = \frac{2.258}{4.539}$ $R^*_{ct} = 4.745$	$R^*_s = .5380$ $R^*_L = \frac{.5306}{1.0686}$ $R^*_{ct} = 1.135$	$R^*_s = .0460$ $R^*_L = \frac{.0459}{.0919}$ $R^*_{ct} = .1004$
1.00	$R^*_s = 2.281$ $R^*_L = \frac{2.281}{4.562}$ $R^*_{ct} = 4.771$	$R^*_s = .5380$ $R^*_L = \frac{.5380}{1.0760}$ $R^*_{ct} = 1.145$	$R^*_s = .0460$ $R^*_L = \frac{.0460}{.0920}$ $R^*_{ct} = .1002$

Table 3.5 Comparison for $R_s^* \simeq 10\, R_L^*$

L/b_L \ x_L	.233	.500	.833
.200	$R_s^* = 22.310$ $R_L^* = \frac{1.772}{24.582}$ $R_{ct}^* = 24.77$	$R_s^* = 5.380$ $R_L^* = \frac{.3830}{5.7630}$ $R_{ct}^* = 5.808$	$R_s^* = .4590$ $R_L^* = \frac{.0407}{.4997}$ $R_{ct}^* = .5104$
.600	$R_s^* = 22.81$ $R_L^* = \frac{2.258}{25.068}$ $R_{ct}^* = 25.35$	$R_s^* = 5.380$ $R_L^* = \frac{.5306}{5.9106}$ $R_{ct}^* = 6.007$	$R_s^* = .4590$ $R_L^* = \frac{.0459}{.5049}$ $R_{ct}^* = .5234$
1.00		$R_s^* = 5.380$ $R_L^* = \frac{.538}{5.918}$ $R_{ct}^* = 5.992$	$R_s^* = .4590$ $R_L^* = \frac{.0460}{.5050}$ $R_{ct}^* = .5235$

Table 3.6 Comparisons for $R_s^* \simeq 0.2\, R_L^*$

L/b_L \ x_L	.233	.500	.833
.200	$R_s^* = .4562$ $R_L^* = \frac{1.772}{2.2282}$ $R_{ct}^* = 2.332$	$R_s^* = .1076$ $R_L^* = \frac{.3830}{.4906}$ $R_{ct}^* = .5091$	$R_s^* = .0092$ $R_L^* = \frac{.0407}{.0499}$ $R_{ct}^* = .0541$
.600	$R_s^* = .4562$ $R_L^* = \frac{2.258}{2.7142}$ $R_{ct}^* = 2.842$	$R_s^* = .1076$ $R_L^* = \frac{.5306}{.6382}$ $R_{ct}^* = .6714$	$R_s^* = .0092$ $R_L^* = \frac{.0459}{.0552}$ $R_{ct}^* = .0603$
1.00		$R_s^* = .1076$ $R_L^* = \frac{.5380}{.6456}$ $R_{ct}^* = .6800$	$R_s^* = .0092$ $R_L^* = \frac{.0460}{.0552}$ $R_{ct}^* = .0600$

3.4 Extension of Model to Include an Interstitial Substance

The investigation has been centered in the past on the study of clean interfaces in vacuum environments. This approach was logical since:

1. The metal-to-metal conduction mode of heat transfer across an interface is the most fundamental. Without a thorough understanding of the metal-to-metal conduction mode, incorrect conclusions could easily be drawn from experimental measurements of interfacial resistances for the combined mode case.
2. The problem is of greater importance in the absence of interstitial conduction since the contact resistance is then much larger.
3. The ability to predict the magnitude of the contact resistance was poorest for interfaces in vacuum environments and the need to know these values was most urgent in this area.

It is felt, however, that a parallel effort on the study of interfaces with the addition of the interstitial conduction mode would be profitable since:

1. The experience which has been gained should prove to be a tremendous asset in the analysis of this closely allied problem.
2. This study might reveal reliable methods of decreasing the magnitude of the thermal contact resistance in a vacuum environment. For example, it could lead to more successful theoretical predictions by giving a method of insuring the lack of importance of microscopic resistances which are, of course, difficult to predict.

3. The study should prove worthwhile in its own right for the following reasons. First, the problem is of interest and importance in other environments as, for example, in nuclear reactor cores, atmospheric operation and testing of space vehicles, etc. Second, satisfactory materials may be developed or may already exist for employment as interstitial substances in vacuum environments for both short and long duration flights. Third, a better understanding of the nature of contacting surfaces and the thermal contact resistance could be obtained from the existing data for interfaces in air if a suitable model were available for the analysis of these data.

The formulation of the problem and a discussion of the solution procedure and results follow.

3.4.1 Problem Formulation and Results of Numerical Calculations

Since the slope of irregularities is usually small, the shape of the irregularities did not enter into the calculation of the thermal contact resistance, in the absence of an interstitial material after the contacting areas were determined. Most of the available models for the determination of the microscopic contact areas are even independent of the asperity shape. The simulation of the flatness deviation by spherical surfaces was employed only as a means of predicting the macroscopic contact area. The distance between the surfaces in the non-contact regions was inconsequential. On the other hand, the shape of the irregularities becomes of primary importance when a substance in the interstices provides a path for the flow of heat across the non-contact regions.

The analysis which follows is valid for either a microscopic or macroscopic protuberance. The assumptions are:

(i) The regions in contact are cylinders of identical radius b; thus, for the microscopic problem a uniform distribution of contact areas is assumed where the region feeding each contact can be approximated by a cylindrical region of radius b.

(ii) The interstitial substance can be treated as a homogeneous, isotropic continuum which completely fills the interstices. The conductivity of this substance is independent of its temperature.

(iii) Natural convection within the interstices is negligible (due to their small dimensions) and conduction within the interstices in a direction parallel to the interface is also negligible.

(iv) The contact is axially symmetrical. The total distance between the contacting surfaces is $f_t(p,r)$ $(0 \leq r \leq b)$. This distance is a function of the initial geometry, the apparent contact pressure, p, and the radial coordinate r. The effect of thermal strain is being neglected but could sometimes be of importance for dissimilar metals in contact (see Ref. 4).

The present problem is seen to be of the same nature at that presented in Section 3.3. The microscopic conductance h_s now becomes $\frac{k_f}{f_t(p,r)}$ where k_f is the thermal conductivity of the interstitial substance. Boundary condition (3.10b) is no longer applicable since the interstitial material provides a conductive path over the complete apparent contact area. The following boundary condition now applies over the entire apparent contact area:

$$k \frac{\partial T}{\partial z} = h(T - T_o), \qquad 0 \leq r \leq b \qquad (3.21)$$

Again, in order to analyze a single region, the interstitial substance must be correctly partitioned. Due to the symmetrical nature of the problem, an isothermal surface exists within the contact. Its temperature is denoted as T_o. The Biot number arises from the boundary condition (3.21). When the interstitial material is correctly partitioned, the Biot numbers of both of the single region problems must be equal and are given by:

$$\frac{h_1 b}{k_1} = \frac{h_2 b}{k_2} = \frac{k_f}{f_t(p,r)} \left[\frac{1}{k_1} + \frac{1}{k_2}\right] b \qquad (3.22)$$

Again the dimensionless contact resistance of both regions will be the same if each is based on its own conductivity. The total dimensionless contact resistance of two dissimilar regions based on their harmonic mean thermal conductivity is simply $R^*_{ct} = 2 R^*_1 = 2 R^*_2$. If the contact were perfect over a portion of the apparent contact area, $f_t(p,r)$ would be zero over this region. Therefore, h would become infinite and the boundary condition (3.21) would simply become an isothermal boundary condition at temperature, T_o.

Examining the boundary condition (3.21) or the appropriate difference equation (3.20), it is seen that an additional parameter enters into the analysis. This quantity follows from Equation (3.22) as:

$$\frac{h_1 b}{k_1} = \frac{k_f}{f_t(p,r)} \left[\frac{1}{k_1} + \frac{1}{k_2}\right] b = 2 \frac{k_f}{k_m} \frac{b}{f_t(p,r)}$$

or introducing dimensionless quantities

$$\frac{h_1 b}{k_1} = 2 \frac{k_f}{k_m} \frac{b}{d_t} f_t^*(\zeta, r^*) \tag{3.23}$$

Thus, for a given geometry, an additional dimensionless parameter arises. It is $(k_f/k_m)(b/d_t)$ and is essentially a Biot number. It will be referred to as the dimensionless interstitial conductance, ψ. It represents a ratio of the conductance of the interstitial substance to the conductance of the internal path, i.e.,

$$\psi = \left(\frac{k_f}{k_m}\right)\left(\frac{b}{d_t}\right) = \frac{k_f A/d_t}{k_m A/b} \tag{3.24}$$

The dimensionless constriction resistance thus becomes a function of

$$R_{ct}^* = g(\zeta, \psi) \tag{3.25}$$

Large values of ψ correspond to a large contribution from the interstitial substance. $\psi = 0$ corresponds to the absence of an interstitial substance, and Equation (3.25) reduces to Equation (3.13), i.e., $R_{ct}^* = g(\zeta, 0) = \phi(\zeta)$.

The solution procedure for this problem is essentially the same as that for the problem of Section 3.3. The difference equation (3.20) is again applicable. In order to obtain the required Biot number, the function $f_t^*(\zeta, r^*)$ must be known. In general, this would require the completion of the extensions to Hertz's analysis which were entertained in Section 3.2. Since these extensions have not been completed, an approximation for this function will be employed. First the case of zero load will be considered since in this case an approximation is not required. The analysis and most of the results presented in this section can be employed in the calculation

of either microscopic or macroscopic resistances.

At zero load, the contact resistance given by Eqaution (3.9) is infinite. Consider now the maximum resistance of such an interface in the presence of an interstitial conductor. Two geometries will be considered--a spherical model and a conical model. An actual microscopic or macroscopic protuberance would probably give a conductance which lies somewhere between the values for these two geometries. For these models the dimensionless distance between the surfaces $f_t(o,r^*)/d_t$ is given by:

$$f_t^*(o,r^*) \simeq r^{*2}, \quad \text{spherical} \tag{3.26a}$$

$$f_t^*(o,r^*) = r^*, \quad \text{conical} \tag{3.26b}$$

The numerical results are presented in figures 3.2 and 3.3. The dimensionless contact resistance which is given represents the total contact resistance for two regions. Some of the curves which are given are not for x equal to zero; thus, they represent the results for finite loads. The following assumptions were made in order to obtain these results:

(i) Perfect contact exists over the area $0 \leq r^* \leq x$; thus, the boundary condition for this region reduces to an isothermal boundary condition since the Biot number is infinite. If one is concerned with macroscopic resistances, this assumption is equivalent to neglecting the microscopic resistances. The assumption for this case is justified in Section 3.4.2.

(ii) Since the variation in the distance between the surfaces with load is unknown, it was assumed that

$$f^*(\zeta,r^*) = (r^* - x), \quad x < r^* \leq 1 \tag{3.27}$$

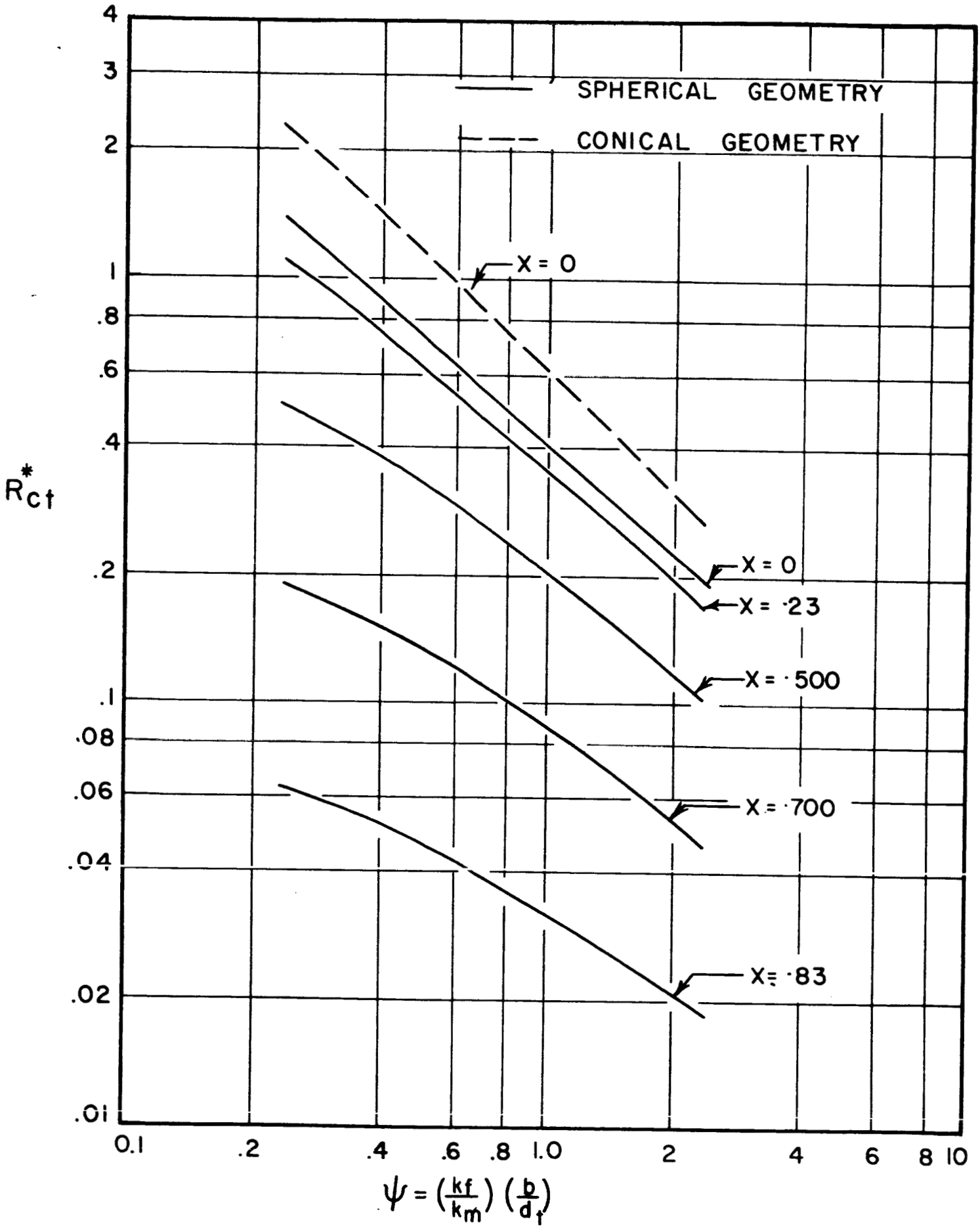

FIG. 3.2 THE INFLUENCE OF INTERSTITIAL CONDUCTION ON THE CONTACT RESISTANCE

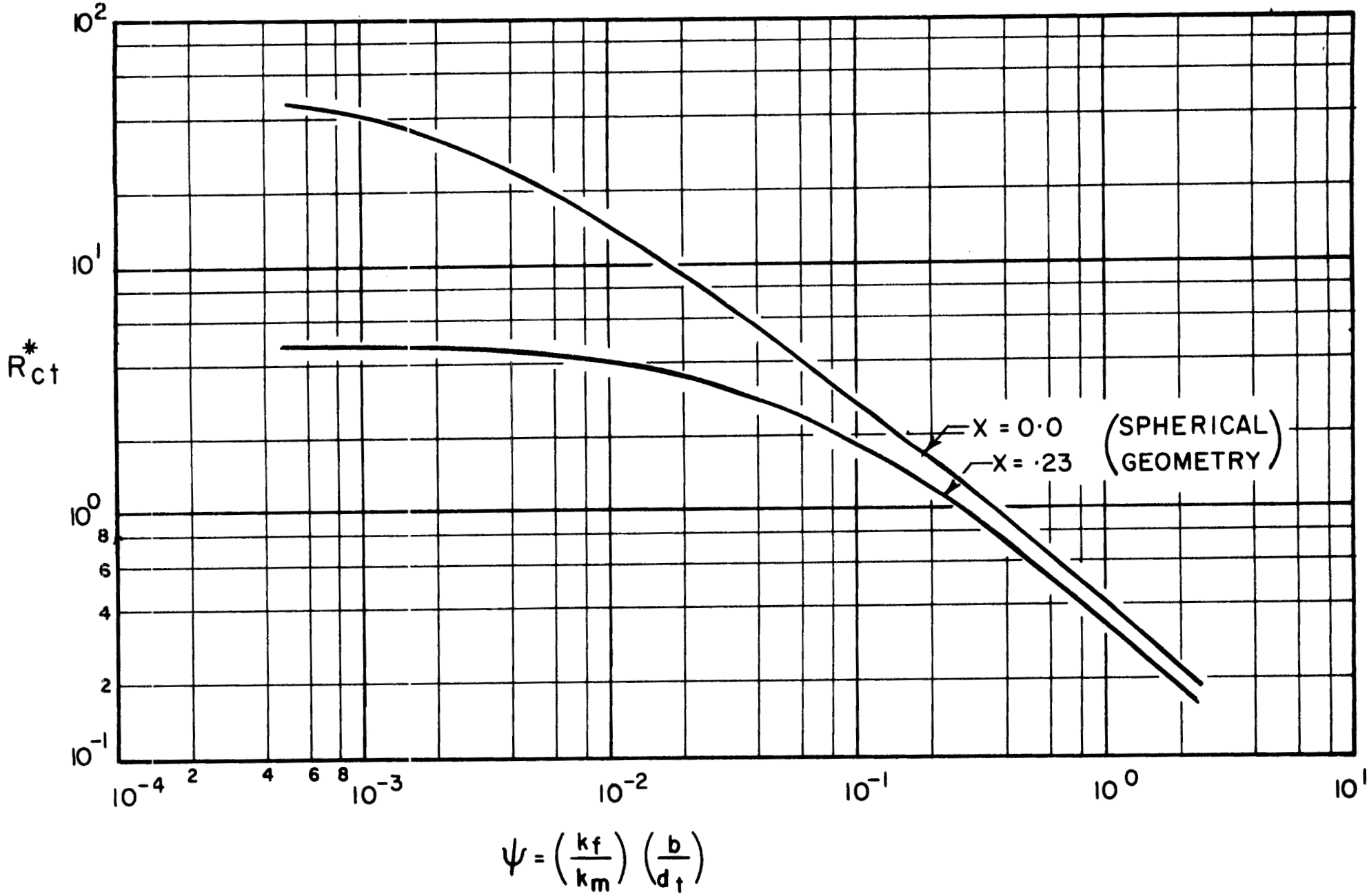

FIG. 3.3 THE INFLUENCE OF INTERSTITIAL CONDUCTION ON THE CONTACT RESISTANCE

where x is a function of the load; hence it is a function of ζ. Equation (3.27) probably gives values of resistances which are too large.

Employing Equation 3.7 to relate the constriction ratio to the load, the results given in Figure 3.4 were obtained. These curves show the variation of the dimensionless constriction resistance with the elastic conformity modulus. The values of the dimensionless interstitial conductance which are given as a parameter cover a range which is thought to be of interest in the study of thermal contact resistances arising from macroscopic irregularities. The results are by no means complete; however, they do clearly indicate:

(i) The significance of the dimensionless interstitial conductance $\psi (= \frac{k_f}{k_m} \frac{b}{d_t})$.

(ii) The large reduction in the thermal contact which can arise with the introduction of an interstitial substance even if it is a poor conductor such as air.

(iii) That one cannot assume the metal-to-metal conduction and the interstitial conduction modes are independent.

(iv) A large error can result if one employs the average distance between the surfaces in calculating the contribution of interstitial conduction even at zero load.

(v) At zero load the average resistance for the conical geometry is approximately 1.5 times larger than the resistance of the spherical model for the range of ψ which was investigated.

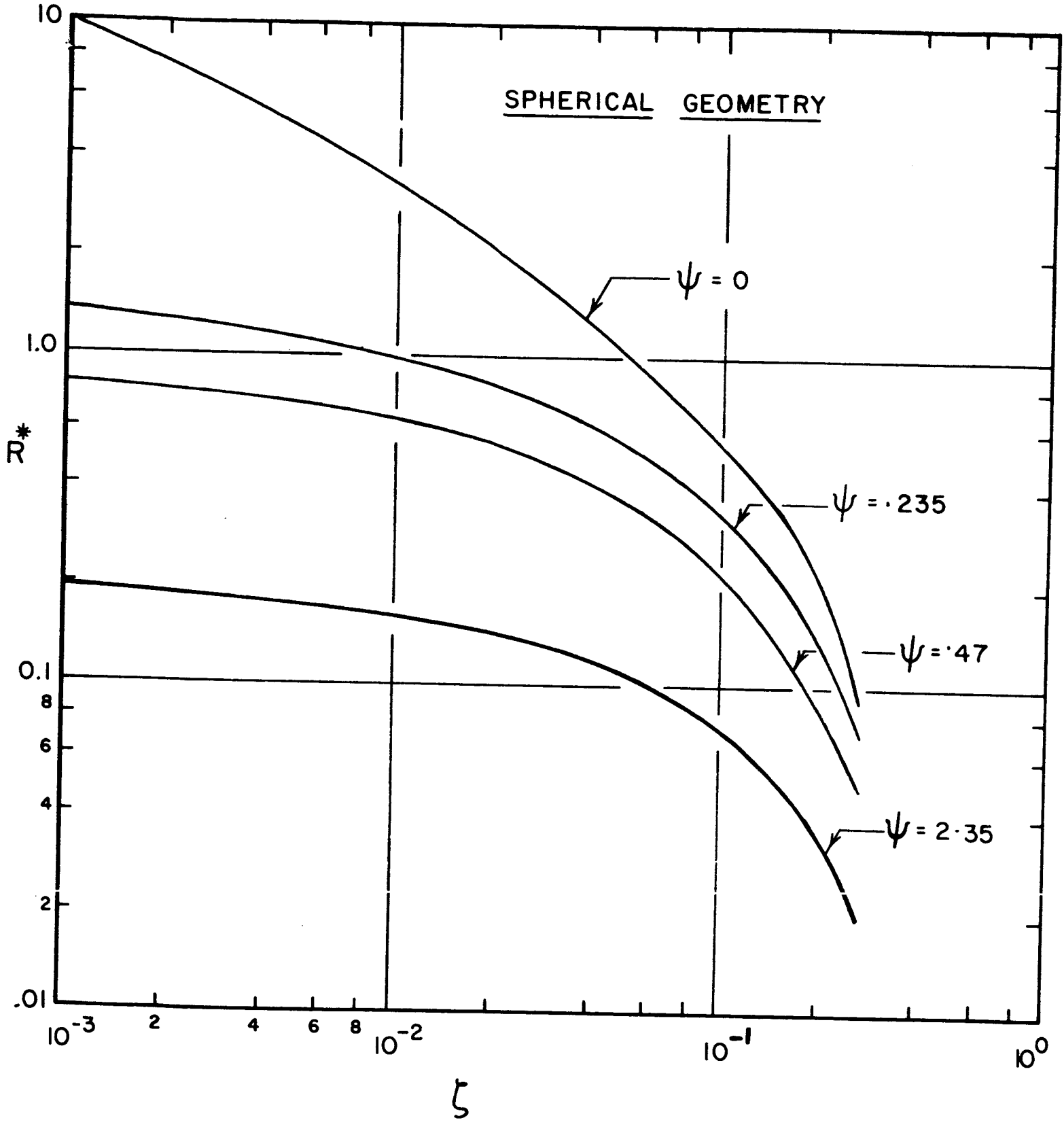

FIG. 3.4 THE INFLUENCE OF LOAD ON THE CONTACT RESISTANCE

3.4.2 Relative Importance of Microscopic Resistances

In the presence of an interstitial conductor, thin surface films appear to offer negligible resistance relative to the constriction resistances. This is because the thermal conductivity of most oxides is not vastly different than the base metal and the thickness of such films is generally small. When an interstitial conductor is present, the flow of heat is no longer confined to the small points of metallic contact; hence thin surface films can be neglected.

In order to compare the nagnitude of the resistance caused by a microscopic protuberance with that caused by a macroscopic protuberance one must first determine the ratios of b/d_t for the two cases. The calculation of b_L/d_{t_L} is rather straightforward; however, it is more difficult to arrive at this quantity for the microscopic roughness.

If one carefully considers profilimeter traces of surface roughness and takes into account the greater magnification in the vertical direction, one sees that the slopes of asperities are not large. The ratio of their base to height is really large in most cases. A limited study of such traces indicates that $2 < b_s/d_{t_s} < 80$.

Employing realistic values of flatness deviation and a ratio of k_f/k_m corresponding to air and aluminum or stainless steel, Figure 3.3 shows that the dimensionless resistance due to a microscopic protuberance could be as much as an order of magnitude greater than the value for a macroscopic protuberance. Now consider the definition of R^*_{ct}: $R^*_{ct} = \Delta L_m/b$ where ΔL_m is the length of material of thermal conductivity k_m whose resistance is equivalent to that of the contact resistance. It is a convenient quantity in this comparison. It is seen that $\Delta L_m = R^*_{ct}\, b$; thus, although R^*_{ct} is larger for a microscopic protuberance, $\Delta L_{m_s} \ll \Delta L_{m_L}$ because $b_s \ll b_L$. Calculations have shown that neglecting the microscopic constriction resistance could cause an error of one percent and in most cases the error is even smaller.

3.5 The Influence of the Region Geometry on the Constriction Resistance--Plane Geometry

3.5.1 Problem Formulation and Results of Numerical Calculations

It is usually assumed that the contact areas which are formed between contacting bodies are circular in nature. For this reason most of the effort expended in the calculation of constriction resistances was concentrated on circular contact areas. The most formidable of these problems is probably that of the finite cylindrical region. This problem was solved by numerical calculations and the results of these calculations were reported in Section 3.2. Interest was recently expressed in two-dimensional plane constrictions [8]. Since the numerical solution procedure recently developed for the axially-symmetrical case was easily modified to the plane problem, it seemed worthwhile to repeat these calculations for the plane case.

The region under consideration is shown in Figure 3.5. The governing differential equation and boundary conditions are:

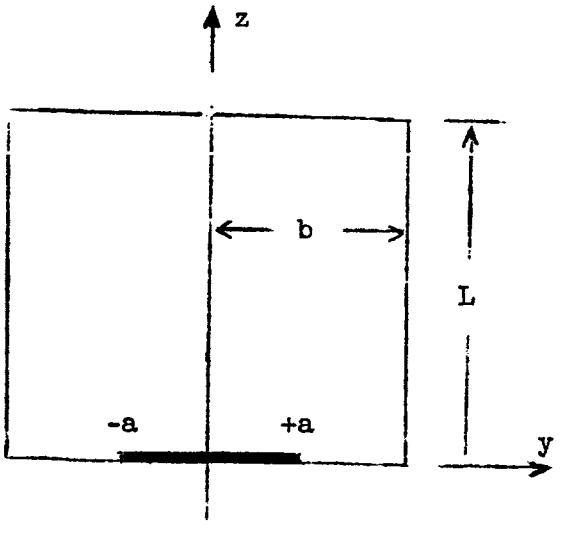

Figure 3.5

$$\frac{\partial^2 T}{\partial y^2} + \frac{\partial^2 T}{\partial z^2} = 0 \qquad (3.28a)$$

$$T(y,L) = T_L, \quad -b \leq y \leq b \qquad (3.28b)$$

$$\frac{\partial T}{\partial y}(\pm b, z) = 0, \quad 0 < z < L \qquad (3.28c)$$

$$\frac{\partial T}{\partial z}(y,0) = 0, \quad \begin{matrix} -b \leq y \leq -a \\ a \leq y \leq b \end{matrix} \qquad (3.28d)$$

$$T(y,0) = T_o, \quad -a < y < a \qquad (3.28e)$$

A differencing procedure similar to that used in [3] was employed in the numerical solution of these equations. The schemes used to speed convergence of the iteration proecdure were also similar. The grid network employed is shown in Figure 3.6. Equal increments were used in the y and z directions. A coarse network was used away from the interface and a fine network was employed near the interface. These networks were joined with triangular elements.

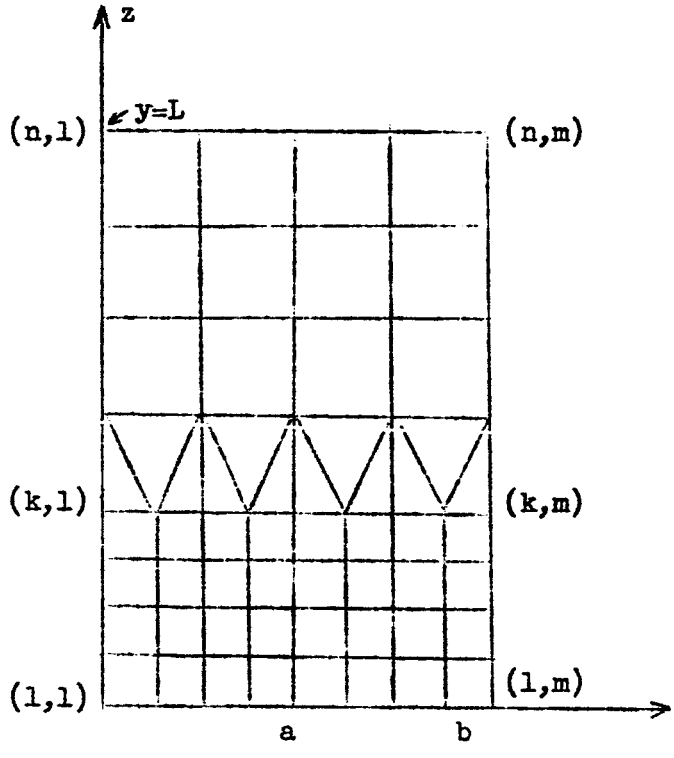

Figure 3.6

Since in the particular solution procedure which was employed, solutions were obtained for two different spacial increments,** an estimate of the truncation error was possible. The error was estimated to be several percent, which is of relatively little importance for a problem of the nature of thermal contact resistance. The exact solution which was later obtained for the limiting case of $L >> b$ showed that the average error was approximately 2%. Since this small error was of little concern, all the numerical computations could be carried out in approximately 8 minutes of production time on the 7094 digital computer.

The results obtained from the numerical solution are reported in Table 3.7. The dimensionless constriction resistance is again employed, $R^* = R\ k\ A_a/b$. It is noted that the dimensionless resistance is independent of the depth of the region since R is inversely proportional to the depth. The resistance given in the table is the constriction resistance of one region only. For two plane regions of the same width and length the total dimensionless resistance is twice the value given in the table. Table 3.8 shows the variation of the ratio $R^*(L/b)/R^*(L/b = \infty)$ with x and L/b. Following the procedures employed for the axially symmetrical case, extensions to include an interstitial substance or the presence of microscopic resistances over the contact area can be easily made.

3.5.2 Exact Solution for the Case of $L >> b$***

Constriction resistance problems are formidable ones due to the presence of the mixed boundary condition along the boundary forming the plane of contact. The boundary is isothermal over the contact area and is a zero flux

---

**17 and 49 columns were employed in the two solutions. The first solution was used as an initial approximation for the second.

***The nomenclature in this section was chosen to conform with standard complex variable nomenclature; consequently, there are several minor conflicts with that employed elsewhere. The complex variables used are: $z = x + iy$; $z' = x' + iy'$; $z'' = x'' iy''$ and $w = u + iv$; therefore, a/b is now used for the constriction ratio instead of the letter x which was previously employed.

$R^* = \Delta L/b$

L/b \ x	.156	.219	.281	.344	.406	.469	.531	.594	.656	.719	.781	.844
0	0	0	0	0	0	0	0	0	0	0	0	0
.250	.6987	.5160	.3928	.3038	.2365	.1838	.1415	.1069	.07814	.05416	.03433	.01852
.375	.8096	.6107	.4710	.3667	.2858	.2213	.1689	.1257	.09010	.06087	.03742	.01953
.500	.8637	.6579	.5107	.3989	.3109	.2400	.1820	.1344	.09521	.06353	.03854	.01986
.625	.8895	.6806	.5300	.4145	.3230	.2488	.1882	.1383	.09763	.06462	.03897	.01999
.750	.9012	.6911	.5389	.4218	.3286	.2530	.1910	.1401	.09866	.06524	.03928	.02007
1.0	.9093	.6983	.5450	.4286	.3325	.2558	.1930	.1413	.09934	.06557	.03941	.02018
1.25	.9110	.6998	.5463	.4279	.3333	.2564	.1935	.1416	---	.06563	---	---
∞	(.911)	(.700)	(.547)	(.428)	(.334)	(.257)	(.1938)	(.142)	(.0997)	(.0657)	(.0395)	(.0202)

Table 3.7 The Dimensionless Constriction Resistance R^* as a Function of x and L/b

$R^*(L/b)/R^*(L/b = \infty)$

L/b \ x/L	.156	.219	.281	.344	.406	.469	.531	.594	.656	.719	.781	.844
0	0	0	0	0	0	0	0	0	0	0	0	0
.250	.767	.737	.718	.709	.708	.715	.730	.754	.784	.823	.869	.918
.375	.886	.873	.861	.857	.856	.862	.872	.885	.903	.928	.947	.967
.500	.948	.940	.934	.932	.931	.931	.939	.946	.955	.967	.975	.983
.625	.976	.972	.969	.968	.967	.967	.971	.974	.979	.983	.989	.990
.750	.989	.987	.985	.985	.984	.984	.986	.987	.989	.993	.994	.994
1.0	.998	.998	.996	.997	.995	.995	.995	.995	.997	.998	.998	.999

Table 3.8 The Ratio $R^*(L/b)/R^*(L/b = \infty)$ as a Function of x and L/b

surface over the remainder of the plane of contact. This suggests that one apply conformal mapping techniques to try to eliminate this mixed boundary condition. These techniques, of course, have only been successfully employed for plane regions; therefore, these methods of solution were not possible for the axially symmetrical case studied in [3].

The boundary conditions of the types given by equations (3.28b) through (3.28e) are invariant with a change of variables arising from a conformal transformation. Therefore the new form of the boundaries is of primary interest. According to Ref. [9] the transformation $z' = \sin z$ transforms the semi-infinite strip into the upper half of the z' plane as shown in Figure 3.7. Two more successive transformations are then applied. The first one $z'' = z'/\sin z$ is a simple magnification by the factor $1/\sin a$. This allows the use of the transformation $w = \sin^{-1} z''$, which is the inverse of the initial transformation. It transforms the upper half of the z'' plane into a semi-infinite strip. It is seen that the initial geometry is again obtained, however, the mixed boundary condition has been removed. The successive transformations which were employed are clearly indicated in Figure 3.7.

The temperature distribution in the w plane is easily seen to be:

$$T = T_o - \frac{q'}{k} v \tag{3.29}$$

where q' is the rate of heat flow per unit depth. To obtain the solution of the original problem, v must be determined as a function of the original variables x and y.

Consider first going from T as a function of v to T as a function of x'' and y''. The transformation is

$$z'' = \sin w = \sin u \cosh v + i \cos u \sinh v$$

Therefore

$$\frac{x''^2}{\cosh^2 v} + \frac{y''^2}{\sinh^2 v} = 1 \tag{3.30}$$

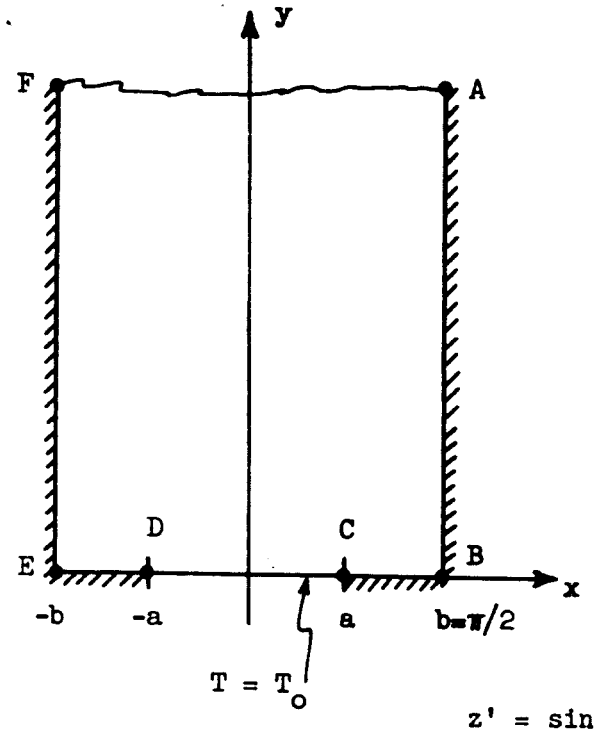

z' = sin z

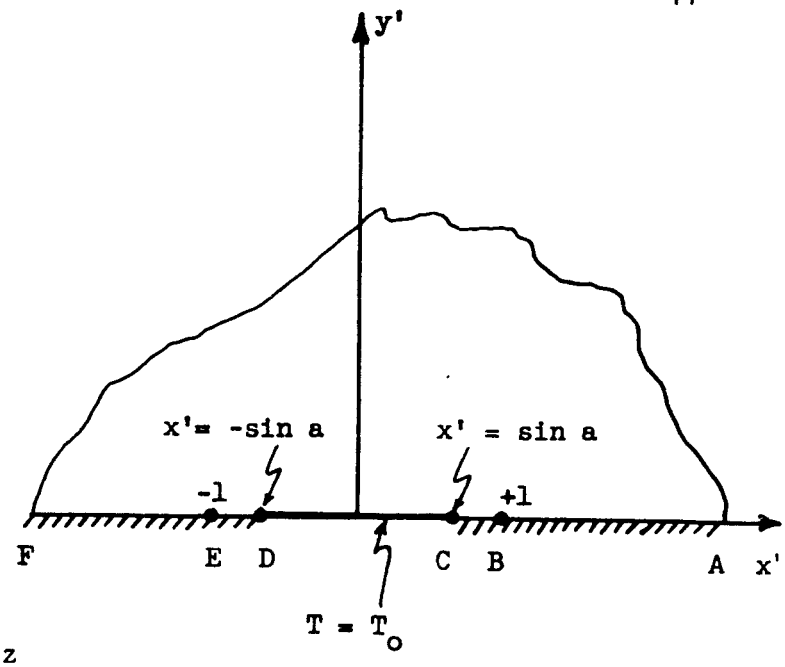

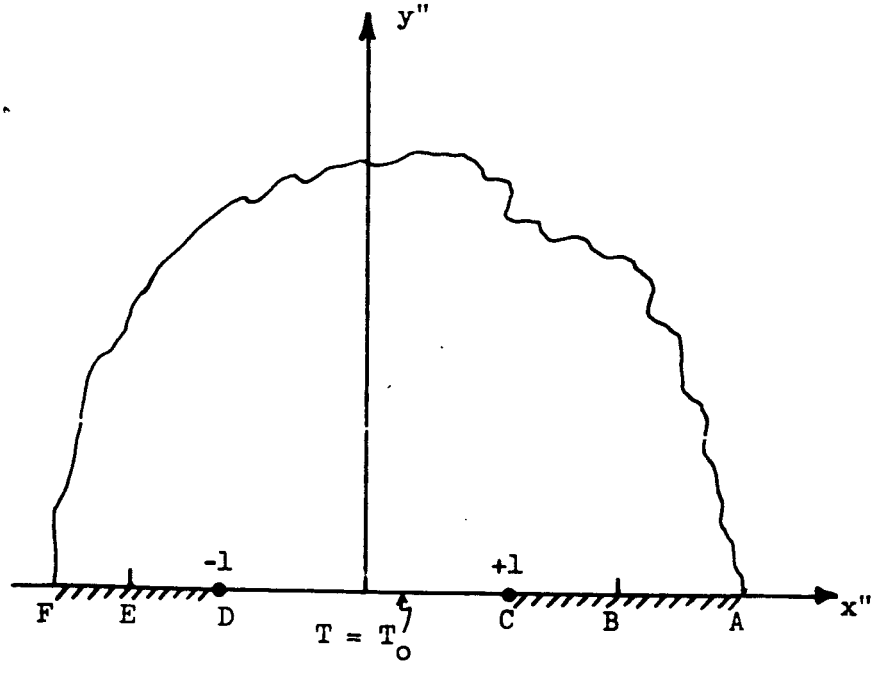

z" = z'/sin a

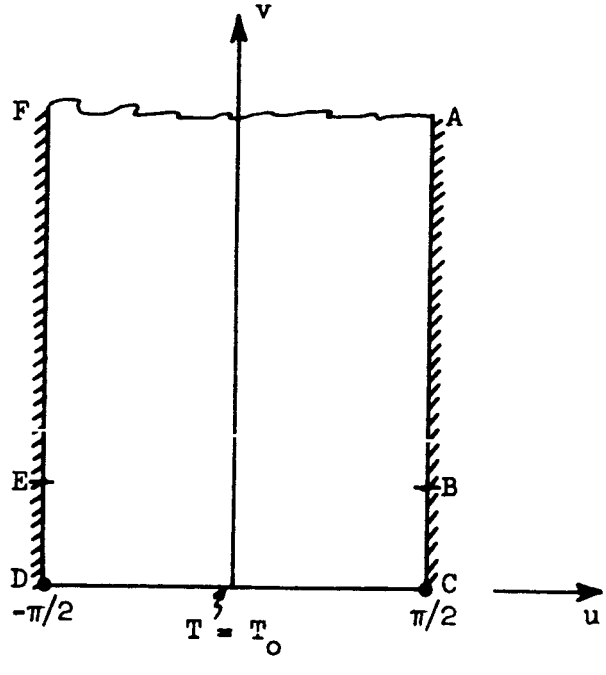

w = $\sin^{-1}$ z"

Fig. 3.7 Successive Transformations Employed

Equation (3.30) shows that the isotherms in the z" plane are ellipses whose centers are at the origin and the foci are at y" = 0, x" $\pm$ 1. From the definition of an ellipse it follows that:

$$2 \cosh v = [(x" + 1)^2 + y"^2]^{1/2} + [(x" - 1)^2 + y"^2]^{1/2}$$

or:

$$v = \ln [Y + (Y^2 - 1)^{1/2}]$$

where:

$$Y = \frac{1}{2}\left\{[(x" + 1)^2 + y"^2]^{1/2} + [(x" - 1)^2 + y"^2]^{1/2}\right\}$$

Also:

$$x" = \frac{\sin x \cosh y}{\sin \frac{\pi}{2}\frac{a}{b}} \quad \text{and} \quad y" = \frac{\cos x \sinh y}{\sin \frac{\pi}{2}\frac{a}{b}}$$

therefore, in terms of the original variables the temperature distribution is:

$$T = T_o - \frac{q'}{\pi k}\left\{\ln [Y + (Y^2 - 1)^{1/2}]\right\}$$

where

$$Y = \frac{1}{2 \sin \frac{\pi}{2}\frac{a}{b}}\left\{[(\sin x \cosh y + \sin \tfrac{\pi}{2}\tfrac{a}{b})^2 + \cos^2 x \sinh^2 y]^{1/2}\right.$$

$$\left. + [(\sin x \cosh y - \sin \tfrac{\pi}{2}\tfrac{a}{b})^2 + \cos^2 x \sinh^2 y]^{1/2}\right\}$$

The constriction resistance is of main interest. It can be obtained by considering a value of $y = y_\infty$ which is sufficiently large such that the temperature is independent of x. The constriction resistance is then given by:

$$R = \left| \frac{[T(y_\infty)|_{a/b} - T_o]}{q'|_{a/b}} - \frac{[T(y_\infty)|_{a/b=1} - T_o]}{q'|_{a/b=1}} \right|$$

If y is very large,

$$T \simeq T_o - \frac{q'}{\pi k} \ln 2Y$$

and

$$Y \simeq \frac{\cosh y}{\sin \frac{\pi}{2}\frac{a}{b}}$$

Therefore:

$$R^* = \frac{2}{\pi} \ln \left\{ \frac{1}{\sin \frac{\pi}{2}\frac{a}{b}} \right\} \qquad (3.34)$$

Equation (3.34) is valid for all possible values of the constriction ratio, a/b; however, it fails to apply if $L/b < 1$ as can be seen from the numerical results given in Table 3.8. Table 3.9 compares the exact solution with the numerical results.

	R^*											
x = a/b	.156	.219	.281	.344	.406	.469	.531	.594	.656	.719	.781	.844
Exact Solution (Eq. 28)	.901	.693	.541	.424	.330	.253	.1909	.1395	.0977	.0643	.0383	.0194
Numerical (Table 5)	.911	.700	.547	.428	.334	.257	.1939	.142	.0997	.0657	.0395	.0202
Percentage Difference	1.2	1	1.1	.9	1.2	1.6	1.5	1.8	2.1	2.2	3.1	4

Table 3.9 Comparison between Exact and Numerical Solutions

4.0 Experimental Facilities and Results

Reference 1 gives a detailed discussion of the experimental facility which was employed in the experimental studies. This reference gives detailed descriptions of: (i) the method which was devised to satisfactorily mount the thermocouples, (ii) the method of preparing the test surfaces and determining their characteristics, and (iii) the procedure employed in the execution of the experimental tests. Reference 2 also gives a brief description of the experimental apparatus and procedure; thus these descriptions will not be repeated in this report. However a brief discussion of the data reduction program which was later written follows and the modifications incorporated in the new experimental facility are given in Section 4.3.

The reduction of the experimental data was a tedious task. The potential accuracy could not be attained due to inherent limitations in the data reduction process. For these reasons, the data reduction scheme was programmed for the 7094 digital computer. Numerous refinements were then incorporated which greatly reduced the error in the results. For example, the thermocouple readings were corrected in order to remove the curvature in the gradients as a consequence of the dependence of the thermal conductivities on the temperature and slight amounts of radiation heat losses. A first degree least squares polynominal approximation was then employed to determine the undisturbed temperature gradient from the corrected thermocoupld readings. This gradient was extrapolated to the test interface. From these extrapolated gradients the additional temperature drop due to the presence of the interface was determined. The differences between the

corrected thermocouple readings and the fitted curve were printed in order to estimate the accuracy and detect the presence of constrictions or erroneous readings. Numerous intermediate results were printed in order to estimate the accuracy of the results.

It is believed that in this fashion high, consistent accuracy was obtained. For example, in some of the low flux tests where high accuracy was required, the thermocouple readings differed from the fitted straight line by less than 0.05 deg F. After all the data were reduced, summary tables were printed and the results were automatically plotted in various manners. The saving in time and labor was tremendous.

4.1 Experimental Verification of the Proposed Model

Extensive results were obtained for contacts between identical materials in order to substantiate the validity of Equation (3.9) or (3.13) in predicting the macroscopic constriction resistance. These results were reported in detail in references 1 and 2. Figure 4.1 of this report summarizes these findings. This figure gives a comparison between the theoretical curve, Eq. (3.9), and the experimental results for all materials investigated. It shows the excellent agreement which was obtained. It also demonstrates the usefulness of the Biot number and the elastic conformity modulus, Y_c, in correlating thermal contact resistance data for materials covering wide ranges of thermal conductivity, elastic modulus, flatness deviation and load.

The experimental results showed some disagreement with theoretical predictions for very small values of flatness deviation. These surfaces were perhaps flatter than those of engineering interest, but the results did

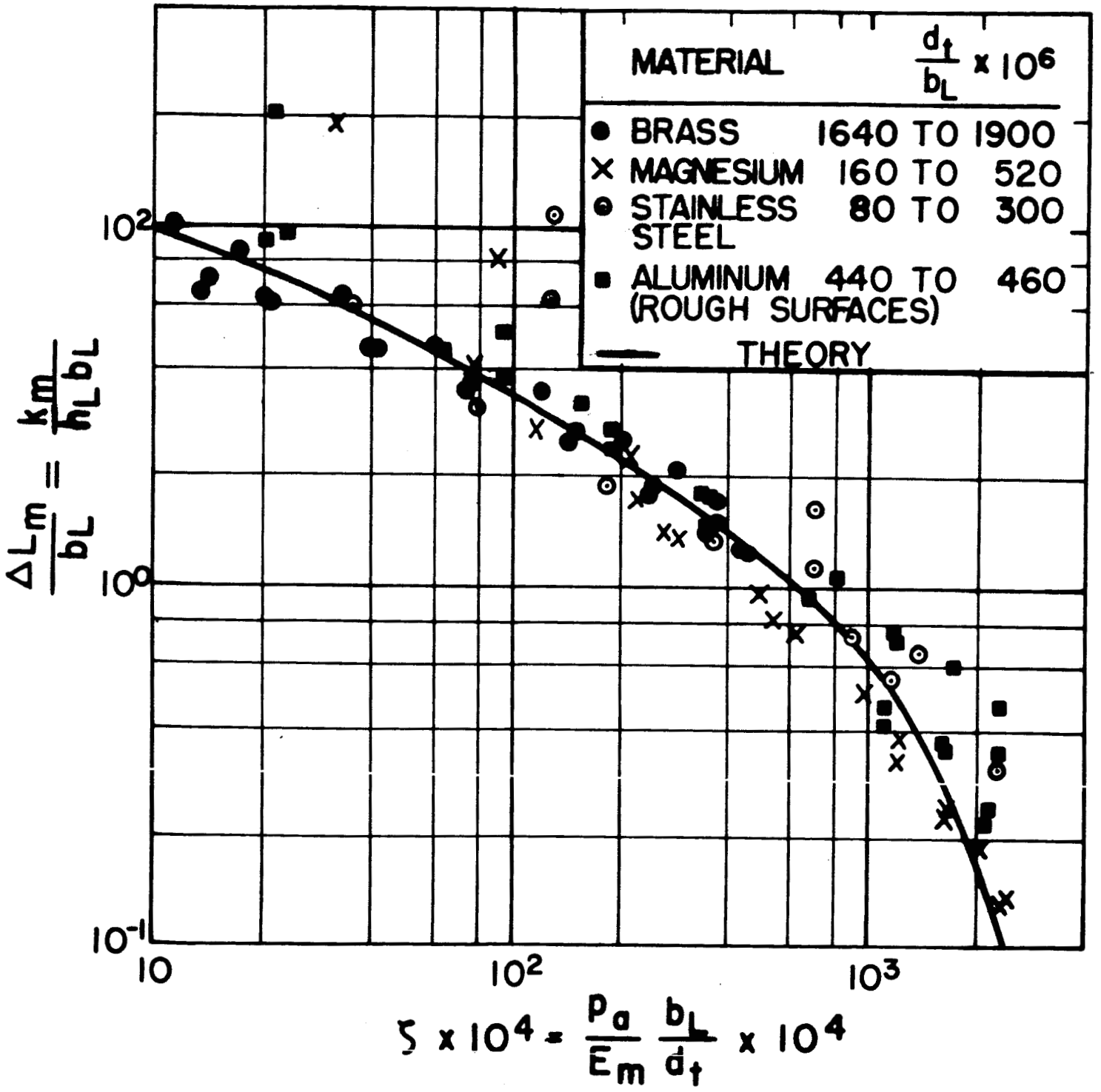

FIG. 4.1 COMPARISON BETWEEN THEORY AND EXPERIMENTAL RESULTS FOR ALL MATERIALS INVESTIGATED

demonstrate that either the effects of thermal strain became important or microscopic resistances were of importance. Many of the results which are discussed in detail in Reference 1 seem to indicate that surface films caused an appreciable resistance and consequently the failure of the applicability of Equation 3.9. A more detailed study of the effects of thin surface films should be made, since conclusive evidence of their importance has not been established.

4.2 An Experimental Study of Dissimilar Interfaces

Several investigations revealed that the thermal contact resistance is influenced by the direction of heat flow in contacts between dissimilar metals. Attempts made in the literature to explain this phenomenon from a microscopic approach were not successful. However, the experimental study which the author conducted and which is reported in detail in Reference 4 showed that the proposed macroscopic model was capable of qualitatively explaining the phenomenon. Quantitative prediction was also possible if the heat flow rates were small.

The expressions derived throughout Section 3 were generalized for application to interfaces between dissimilar metals. However, it was also stated that they were valid for dissimilar metals only if the effects of thermal strains were negligible. The basis for this can be seen from the following auguments.

It can be seen from Figure 4.2 that if heat is flowing from region 1 to region 2, i.e., in the direction 1-2, the portion of region 1 near the macroscopic contact area is cold relative to the rest of the member. Thus, this portion contracts, which causes the formation of a larger macroscopic

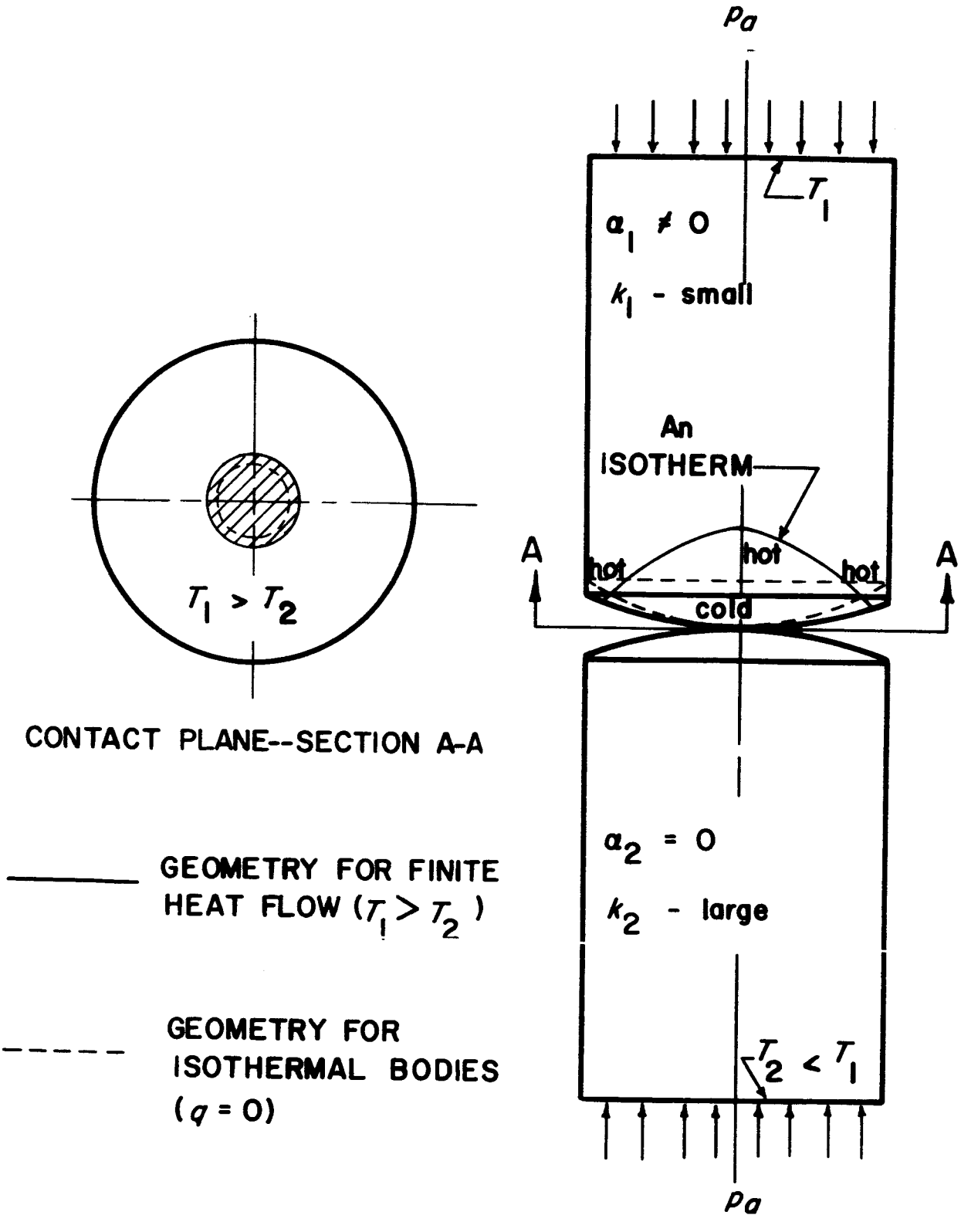

FIG. 4.2 GEOMETRIC EFFECTS OF THERMAL STRAIN RESULTING FROM A MACROSCOPIC CONSTRICTION

contact area than that which is predicted if only the mechanical stresses are considered (see Fig. 4.2). If the direction of heat flow is reversed, the portion of region 1 near the macroscopic contact is hot relative to the remainder of the member. In this case, the thermal strain causes a smaller macroscopic contact area than that which is predicted from the mechanical stresses. Thus, it is seen that if the heat is flowing in the direction 1-2, the thermal strain causes a decrease in the macroscopic constriction resistance, whereas if it is flowing in the direction 2-1, the thermal strain causes an increase in the macroscopic constriction resistance. The thermal contact resistance thus becomes a function of the direction of heat flow.

The geometry of the contacting members will obviously influence the size of the macroscopic contact area and the manner in which the size of this area varies with the mechanical load. However, the trend of the directional effect is seen to be independent of the geometry of the contacting surfaces. For example, consider the case when the heat is flowing in the direction 1-2. The portion of region 1 near the macroscopic contact area will be cold relative to the surrounding portion of the region. The thermal strain for this case will cause the macroscopic contact area to grow whether the upper contacting surface is concave or convex. (The lower surface could also be either concave or convex.)

The amount of thermal strain which occurs is a function of the coefficient of linear expansion α, the modulus of elasticity E, Poisson's ratio ν, and the magnitude of the temperature gradients. Thus the influence of thermal strain is dependent on the heat flux and the thermal conductivity of the material. If the heat flux is small and the thermal conductivity is large, the influences of thermal strain would vanish.

Now, consider a contact formed between two identical materials where both the upper and lower regions have the same coefficient of linear expansion. If the material properties are independent of temperature, the thermal strains perpendicular to the interface which occur in the regions as a consequence of macroscopic constrictions are complementary; thus, the macroscopic contact area is approximately the same as that present in the absence of thermal strain. Since the variation of the material properties with temperature is not large, the neglect of the effect of thermal strain due to macroscopic constrictions should not cause much discrepancy between the theoretical predictions and the experimental results for contacts between identical materials. Dependency of material properties on temperature will not cause a directional effect in contacts between identical materials as long as the specimen's geometries and the imposed boundary conditions are identical.

The curves given in Figure 4.3 show the variation of the contact resistance with heat flux at constant load for a stainless steel-aluminum interface. The three curves given are for contact pressures of 44.6, 86.9, and 157 psi. The arrows on the curves indicate the order in which the data were taken. It is seen in these figures that as the heat flux approaches zero, the directional effect vanishes.

Although the thermal strain due to the macroscopic constriction seems to dominate these experimental results, it is believed that another effect can be seen--thermal strain due to the thermal environment. Small gradients in a direction parallel to the plane of the interface can cause an appreciable change in the macroscopic constriction resistance. These gradients in this

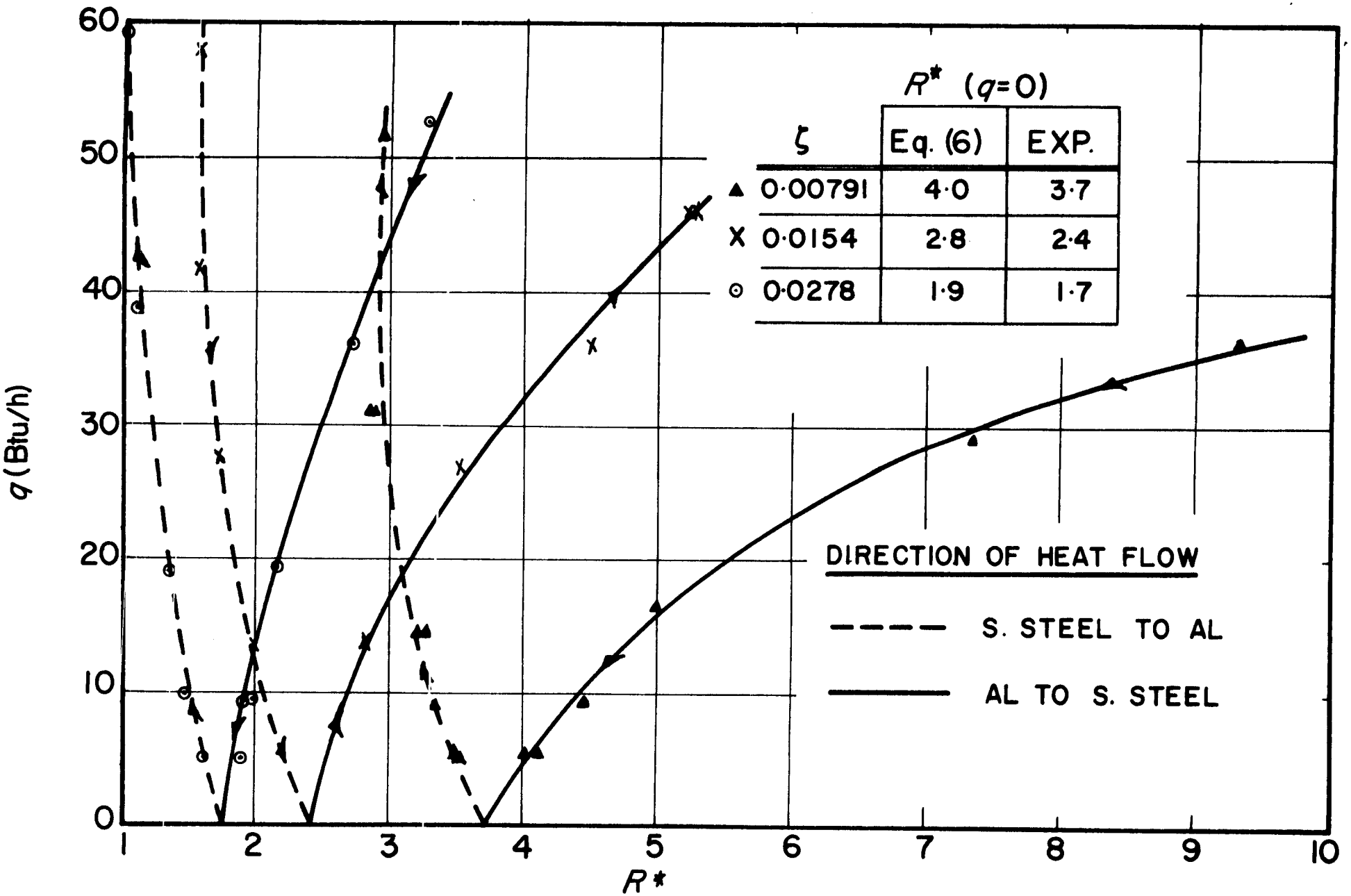

FIG. 4.3 THE INFLUENCES OF THE RATE OF HEAT FLOW, DIRECTION OF HEAT FLOW, AND CONTACT PRESSURE: STAINLESS STEEL-ALUMINUM INTERFACE (d_t = 180 μIN.)

case arise from small amounts of radiant heat lost from the specimen's surfaces. Other possibilities are heat exchange with the environment due to the surrounding insulation , a surrounding gas, an alignment device, etc. Many of these environments would be of greater significance than the small amount of radiant heat loss from the highly polished surfaces in the present investigation. The directional effect arises with dissimilar metals due to changes in the temperature levels of the specimens with the direction of heat flow. It is seen that this source of thermal strain may be beneficial or detrimental depending on the original geometry of the surfaces and on the sign of the radial heat flux. For the geometry employed in the present investigation, the effect was always detrimental since the specimens were losing heat by radiation to the chamber walls in all cases.

It is believed that this effect can be detected in the data of Figure 4.3. For example, the change in the dimensionless resistance R^* with the rate of heat flow q; i.e., dR^*/dq, is either positive or negative depending on the direction of heat flow; however, d^2R^*/dq^2 is always positive. The fact that d^2R^*/dq^2 is always positive is probably due to the radiation heat losses. Figure 4.3 also shows that for the case when heat flowed from stainless steel to aluminum, dR^*/dq approached zero for large values of q. Perhaps if q were sufficiently large, the thermal strain due to heat losses would dominate, and dR^*/dq would be positive.

A comparison is given in Figure 4.3 between the experimental values extrapolated to zero heat flow and the theroetical prediction of Equation (3.13). The two values agree to within approximately 10%. This is believed excellent considering the nature of the problem. It is seen that the

theoretical predictions are larger than the experimentally measured resistances. This is probably a consequence of an increase in the conformity of the specimens during the test series due to the creep of the aluminum specimen. Flatness measurements taken after completion of the test series showed the aluminum specimen had a "hole" at the center portion of its surface which was approximately 6μ in. deep. Further data and discussion of the directional effect is given in Reference 4.

4.3 The New Experimental Facility

The experience gained from the use of the old experimental facility indicated several major improvements which could be made. In addition the theoretical results suggested other aspects of the problem which should be investigated; however, the old facility was not designed for these extensions. Therefore, it was decided profitable to design and construct a new experimental facility. The main differences between this facility and the old one will be described.

The old chamber was a cylinder with a 6 in. inner diameter and a height of approximately 12 inches. Its small size proved to be a handicap especially due to the problems involved in changing and aligning the specimens. Its size also made the addition of guards virtually impossible. The new chamber was enlarged to an inner diamters of 12 in. and a height of 15-1/4 in. A second cylindrical section of 8 in. inner diameter was inserted in the side as is shown in Figure 4.4. The specimens can be easily changed by only removing this one flange (see Figure 4.4). With this design the specimens can be aligned accurately by hand with no need for an elaborate device and

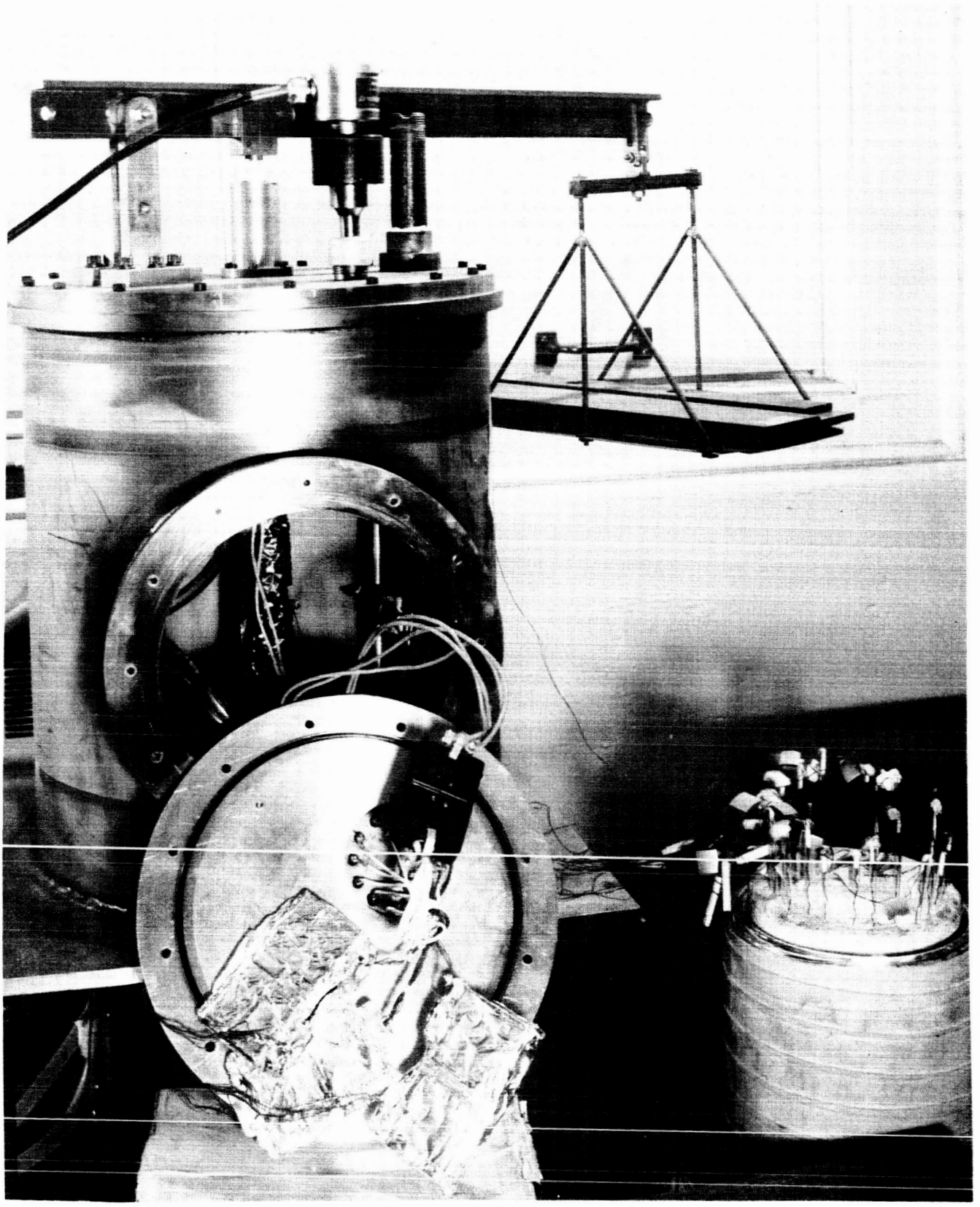

FIG. 4.4 GENERAL VIEW OF TEST CHAMBER

no possibility of a thermal shunt due to the presence of such a device. In changing the specimens the sink and source can be left essentially in place and their many connections need not be disturbed. A general view of the complete facility is given in Figure 4.5.

The dead-weight loading system, a very desirable feature, was retained; however, several modifications to the old design were incorporated to reduce the effects of friction. The bushing around which the level arm rotated was replaced by a roller bearing and the bushing which guided the loading pin was replaced by a precision longitudinal bearing. Thus, the effects of frictional loading which were found to be small in the old design were virtually eliminated in the new facility. The rectangular cross-section of the old lever arm was changed to a T-section to reduce its laterial motion. The loading system can be clearly seen in Figure 4.4.

Other changes were made to reduce the loading caused by the cooling water lines and to reduce the heat losses. Guards were designed so that the radiation heat loss could be eliminated or if the effects of such radial heat flow were being studied, to enable its control. These devices have not yet been successfully employed.

The AC power source for the heating element was replaced by a well regulated DC constant voltage supply. The voltage was varied by means of a rheostat. Figure 4.6 gives a schematic diagram of the experimental facility.

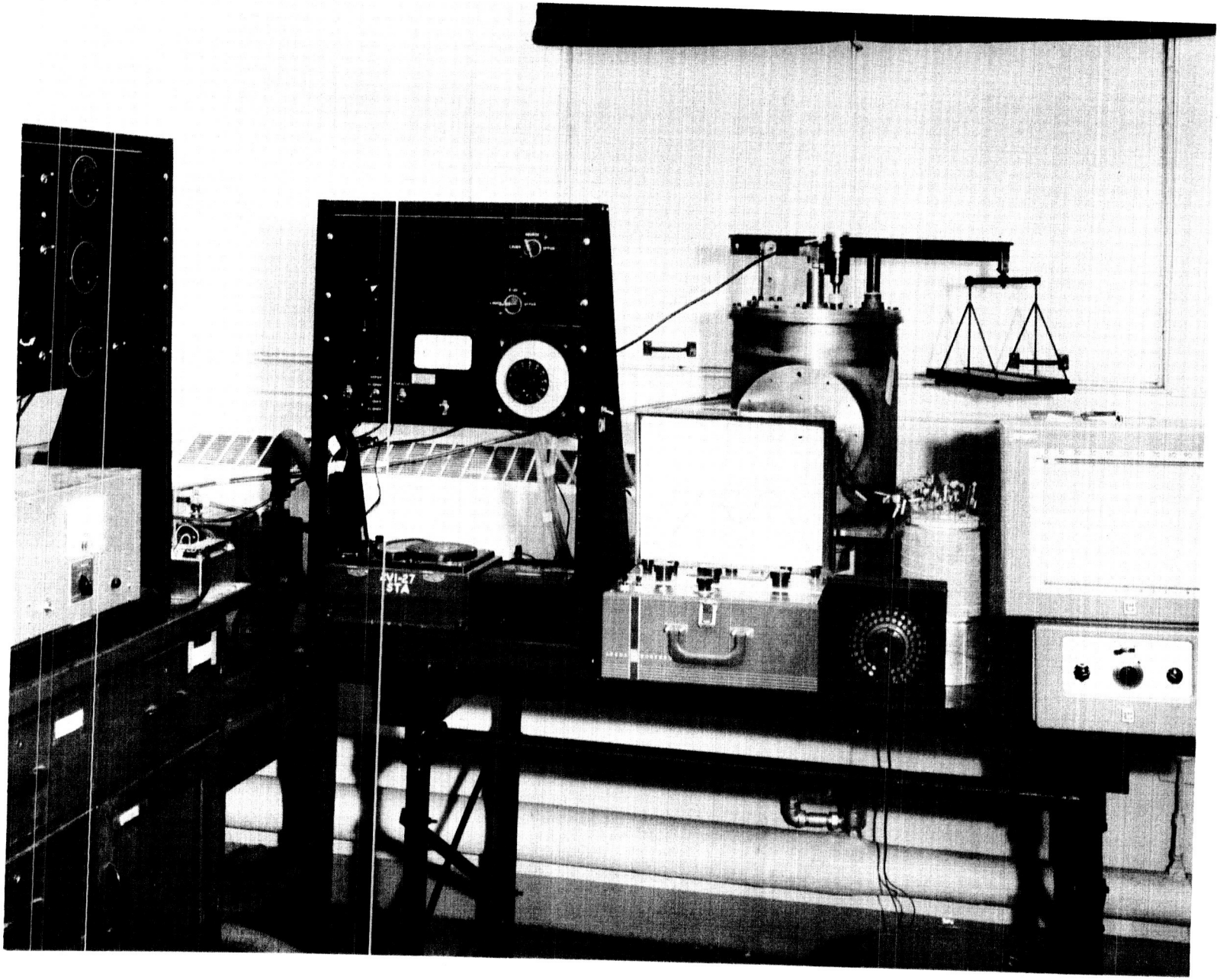

FIG. 4.5 GENERAL VIEW OF EXPERIMENTAL SYSTEM

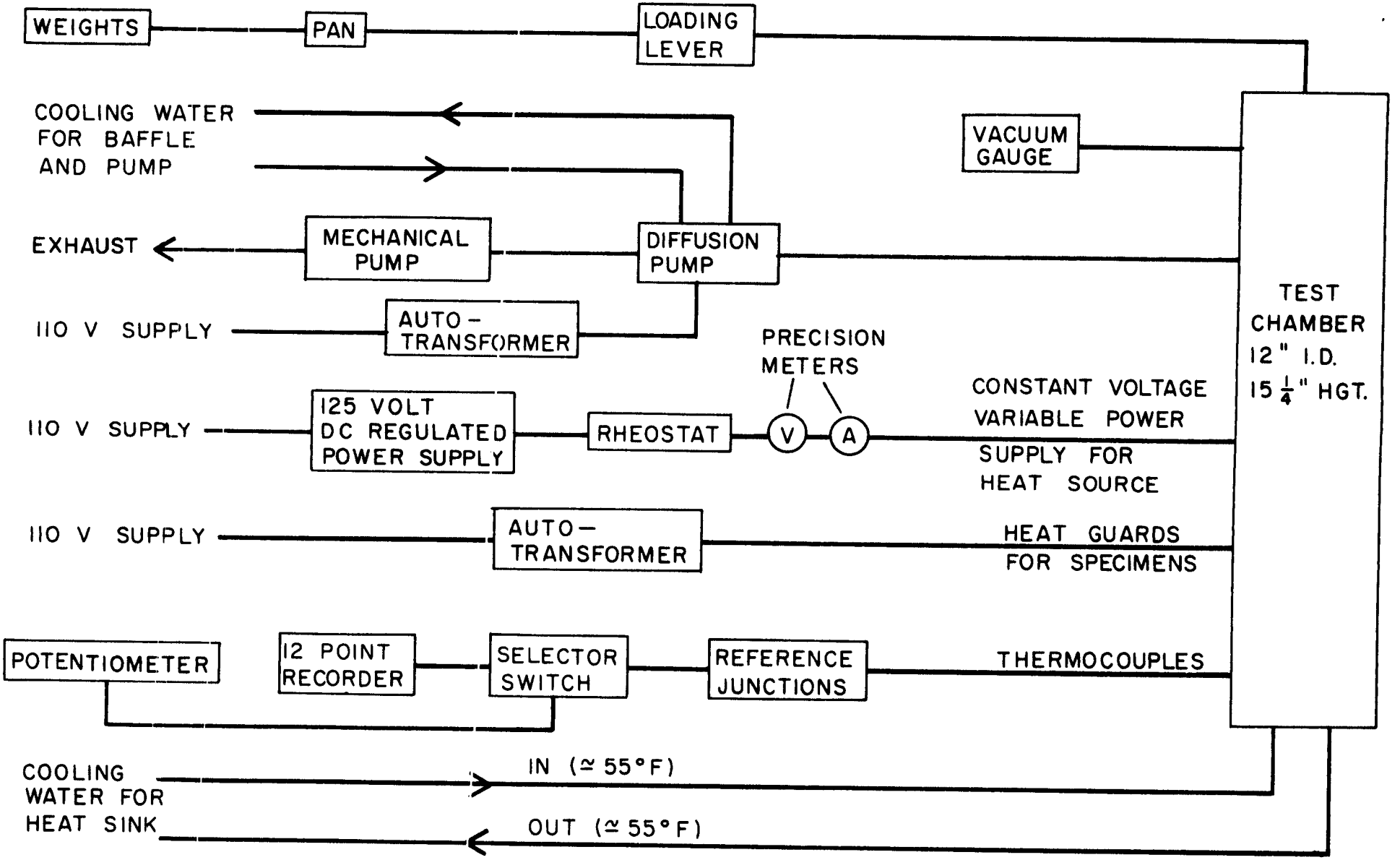

FIG. 4.6 SCHEMATIC DIAGRAM OF EXPERIMENTAL FACILITY

5.0 Summary and Conclusions

A restrictive analysis based on a new macroscopic model was presented for the prediction of the thermal contact resistance in a vacuum environment. The thermal contact resistance was conceived to be a consequence of three resistances in series: the macroscopic constriction resistance, the microscopic constriction resistance, and the film resistance.

Preliminary calculations showed that the macroscopic resistance was of major importance and the emphasis of the analysis and experimental study was to further the understanding of thermal contact resistance by obtaining a better understanding of macroscopic influences. The model was also extended to include an interstitial substance.

The following major conclusions could be drawn based upon conditions within the limits of this investigation:

1. Macroscopic influences are of major importance and dominate the thermal contact resistance of a majority of engineering surfaces. This fact has been grossly overlooked in many previous investigations.
2. An analysis based on a model of macroscopic elastic contact between mating members has been carried out, which makes possible a satisfactory prediction of thermal contact resistance whenever the macroscopic constriction is dominating and the effects of thermal strain are small. It naturally leads to a pair of dimensionless parameters for correlating data. They are:

   the Biot nodulus: $\dfrac{h\, b_L}{k_m}$

   and

   the elastic conformity modulus: $\gamma = \left(\dfrac{p_a}{E_m}\right)\left(\dfrac{b_L}{d_t}\right)$

Experimental evidence is given to establish the validity of the theory. The extension which includes an interstitial conductor resulted in a third dimensionless parameter, the dimensionless interstitial conductance: $\psi = (\frac{k_f}{k_m})(\frac{b}{d_t})$.

3. Evidence was given to demonstrate that thermal strain due to macroscopic influences can cause a pronounced directional effect in contacts between dissimilar metals. The proposed model was found to be capable of predicting the thermal contact resistance for interfaces between dissimilar metals if the effects of thermal strain were not of importance which is often the case with small rates of heat flow.

4. Film resistance can be of considerable importance for heavily oxidized surfaces in the absence of an interstitial substance; however, it was found that for freshly machined surfaces with a realistic value of flatness deviation, film resistance is of secondary importance. The analysis which includes an interstitial conductor shows that the effects of microscopic resistances can surely be neglected (even with a poor interstitial conductor such as air) with realistic, freshly machined contacts.

5. The model with its resulting dimensionless groups, $\frac{h\, b_L}{k_m}$, $(\frac{p_a}{E_m})(\frac{b_L}{d_t})$ and $(\frac{k_f}{k_m})(\frac{b}{d_t})$, clearly indicates the effect of the many parameters and provides a means of designing high or low resistance interfaces. It clearly indicates both when accurate predictions are possible and when accurate predictions would be difficult.

6. The reduction in the contact resistance with the inclusion of an interstitial substance is appreciable even with a poor interstitial conductor such as air. The magnitude of $(\frac{k_f}{k_m})(\frac{b}{d_t})$ clearly indicates the importance of interstitial substances.

7. The macroscopic constriction resistance, the microscopic constriction resistance, and the film resistance cannot be calculated independently if more than one of these resistances are important. Likewise, the interstitial conduction mode and the metal-to-metal conduction mode cannot be calculated independently. Lastly, the macroscopic and microscopic contact areas cannot, in general, be calculated without simultaneously considering the thermal problem.

6.0 Recommendations for Future Extensions

The present investigation has porvided a better understanding of the mechanism of thermal contact resistance. It has revealed the importance of macroscopic effects and has been successful in predicting the thermal contact resistance for the restrictive model being studied. As usual, there still remain numerous extensions and refinements to be undertaken. It is believed that the present model, the experimental results which were obtained, and the numerical calculations which have been performed, will provide a solid basis from which further studies can be effected. A few recommended extensions follow.

Perhaps the most useful extension, especially to those who are involved with thermal design, would be to attempt to employ the results of this study to correlate the experimental results from other investigations for interfaces with and without an interstitial conductor. This study has provided meaningful dimensionless parameters for such a correlation and has revealed the relative importance of many of the variables. If a more complete study of the characteristics of surfaces manufactured by various production processes were made and these findings utilized to obtain the required parameters, the model could perhaps be successfully adapted to this worthwhile endeavor.

This study has provided a means of predicting the thermal contact resistance when an interstitial substance is present; however, this aspect of the theory has not been experimentally verified. An experimental study of interfaces with an interstitial substance in the light of the present analysis would be desirable. The investigation of substances such as lead foil or other readily deformable materials might be included in this experimental

study. It would be interesting to learn if an interstitial substance could be found which is suitable for extended employment in a vacuum environment and at the same time is sufficiently well behaved such that its influence could be accurately predicted.

Although all the results of the present investigation indicate that the microscopic constriction resistances are not of importance, conclusive evidence has not been obtained. Further experimental studies are necessary to substantiate this conclusion. On the other hand, film resistance was found to be of importance in some cases for interfaces in the absence of an interstitial substance. Methods of reducing the film resistance should be investigated. For example, plating the contacting surfaces with a noble metal such as gold or silver may provide a means of reducing film resistance.

Another area which would be a logical extension of this study would be the investigation of the influences of constriction resistances in the transient heat exchange between bodies. Preliminary calculations have shown that the time required for two members to exchange a given amount of energy with a non-perfect contact between them could easily be an order of magnitude greater than the time required to exchange the same amount of energy with perfect contact.

Extensions to the deformation model to increase its range of applicability and to include the effects of thermal strain were already discussed in Section 3.2 and, as was stated there, are partially completed.

The extensions which have been listed are but a few of the many interesting problems which could be studied. They are presently thought to be some of the more fruitful and worthwhile endeavors.

7.0 References

1. A. M. Clausing, "Thermal Contact Resistance in a Vacuum Environment," Ph.D. Thesis, University of Illinois, August, 1963 (see also Univ. of Ill. Eng. Exp. Station Report, ME-TN-242-1).

2. A. M. Clausing and B. T. Chao, "Thermal Contact Resistance in a Vacuum Environment," ASME J. of Heat Transfer, Vol. 87, 1965, pp. 243-251.

3. A. M. Clausing, "Some Influences of Macroscopic Constrictions on the Thermal Contact Resistance," Univ. of Ill. Eng. Exp. Station Report, ME-TN-242-2, April, 1965.

4. A. M. Clausing, "Heat Transfer at the Interface of Dissimilar Metals--The Influence of Thermal Strain," Int. J. Heat Mass Transfer, Vol. 9, 1966 (at press).

5. H. Atkins, "Bibliography on Thermal Metallic Contact Conductance," NASA TM X-53227, 1965.

6. L. C. Roess, "Theory of Spreading Conductance," Appendix A of an unpublished report of the Beacon Laboratories of Texas Company, Beacon, New York.

7. R. Holm, Electrical Contacts Handbook, Springer Verlag, Berlin, 3rd Ed., 1958.

8. Personal correspondence with Dr. John Lucas, Jet Propulsion Laboratory and with Mr. M. Yovanovich, Mass. Inst. of Technology.

9. R. V. Churchill, Complex Variables and Applications, McGraw-Hill, New York, 1948, p. 207.